Coordination of power flow control by using FACTS device and HVDC transmission system

A thesis submitted to Cardiff University in partial fulfilment of the requirements for the degree of MPhil

School of Engineering, Cardiff University

September, 2016

Student name: Xiaotian Wang

Student number: 1149499

Abstract

UK government has set the ambitious decarbonisation targets, which up to 30GW of wind generation could be connected to the GB transmission system before 2020. The majority of the new wind generation will be in the Scotland, and offshore in the UK as a whole, where the maximum levels of wind resource are available. To fully use the generated power from wind farm, the higher power transfer capacity of transmission system is required. A range of new transmission technologies such as Thyristor Controlled Series Compensation (TCSC) and embedded High Voltage Direct Current (HVDC) link are planned to reinforce the GB system in order to increase the transmission capacity and improve the oscillatory behaviours. This thesis investigates the effectiveness of this two power flow control devices to enhance the transient stability of the GB power system. A coordinated controller to maximise the effect of TCSC and HVDC link is proposed and designed. The power system can operate at optimal operational point after fault due to setting the appropriate dispatched proportion of controller. The best performance is achieved by comparing various study cases. Meanwhile, the principle to dispatch the power flow is studied and presented in the thesis.

Acknowledgement

First and foremost, I would like to show my deepest gratitude to my supervisor, Dr. Jun Liang, for the help he gave to me and the time he spent for me, even on weekends. Meanwhile, I would like to show my grateful feeling to my family, for their support.

Contents List

Chapter One: Introduction

The rapid development of power systems generated by increased demand for electric energy initially in industrialized countries and subsequently in emerging countries led to different technical problems in the systems. Development based on semiconductor devices first established High Voltage Direct Current (HVDC) transmission technology as an alternative to long-distance AC transmission. HVDC technology, in turn, has provided the basis for the development of Flexible AC Transmission System (FACTS) equipment which can solve problems in AC transmission.

In UK, the majority of the new wind generations will be in Scotland which would result in significant increase in power transfer capability requirement between the Scottish Power Transmission (SPT) and National Grid Electricity Transmission (NGET) boundary. A potential solution to provide the required increase in transfer capacity in order to support the additional generation is to deploy state-of-the-art transmission technologies such as Thyristor Controlled Series Compensation (TCSC) and embedded HVDC links as alternatives to traditional system reinforcements. These two kinds of power flow controller devices could dynamically change the overall structural and oscillatory behaviour of the system and consequently affect the system stability. Due to with different characteristic and advantage for enhancing the power system, both of two technologies are going to be applied together. Therefore, a coordinated control method is needed to guarantee the optimal dynamic performance for the coordination of power flow control.

The research question is to investigate how to achieve optimal operational point to enhance the transient stability of GB power system when TCSC and HVDC regulate power flow concurrently. In order to solve the question, several objectives have been achieved and presented in this thesis:

- Identify the requirement of the National Grid power system.
- Build the models of new transmission technologies (HVDC and TCSC) which is planned to reinforce the GB system.
- Investigate the performance of the coordinated operation of HVDC and TCSC with regards to the transient stability enhancement.

- Develop and analyse a coordinated control system of two devices to guarantee the robustness and stability of power system under varying operational conditions.

In Chapter 2 a general overview of HVDC transmission technology is presented with description of the coordination of LCC-HVDC and various types of FACTS devices. In addition, several coordinated control methods are summarized. In Chapter 3 LCC-HVDC and TCSC model with overall control system is built in Advanced Digital Power System Simulator (ADPSS). To study the characteristics and validate parameters of control systems of models, several step-change tests are illustrated. In Chapter 4 the power flow controller is added into LCC-HVDC control system which is applied with TCSC to improve the transient stability of the simplified GB power system at post-fault. The simulations of coordinated operation of these two power control devices are studied and analysed. In Chapter 5 a coordinated controller for dispatching power flow is designed to achieve the optimum coordination of power flow control. The power system operates at optimal operational point after fault because of the appropriate dispatched proportion which is set in coordinated controller. Chapter 6 concludes the research work and proposals for further work are made. References and appendices are shown in the end of thesis.

Chapter two: Literature Review

2.1 Introduction

High Voltage Direct Current (HVDC) has many advantages in power transmission which is widely used to transmit large amounts of power over long distances. A Flexible Alternating Current Transmission System (FACTS) is a system composed of static equipment used for the AC transmission of electrical energy [1]. FACTS devices are used to provide flexible power flow control, support system voltage and improve stability. Multiple FACTS devices in cooperation of HVDC links can greatly improve system performance. However, there are interactions between FACTS and HVDC which could cause unexpected adverse impact on operation system. Proper coordination of HVDC links and FACTS devices embedded within AC system is a new urgent research topic.

2.2 HVDC

2.2.1 Comparison of AC-DC transmission

HVDC is an efficient technology for long distance power transmission. It can replace the AC transmission between two grids. The advantages of the two methods of transmission (AC and DC) which should be considered by designer are based on the following factors [2]:

- Economics of power transmission
- Technical performance
- Reliability

The increased power demand makes power system expansion important. This means that the construction of a transmission line must be considered as a part of a long term planning.

a. Economics of power transmission

The cost of a transmission line includes the capital investment required for the actual infrastructure (i.e. Right of Way (RoW)), towers, conductors, insulators and terminal equipment and costs incurred for operation.

Assuming the insulator characteristics, which depends on the peak voltage level applied with respect to ground, are similar for AC and DC. DC transmission can transfer more power at a given voltage level than AC transmission due to only passing active power. In addition, a DC line can carry as much power with two conductors as an AC line with three conductors of the same size [3]. Therefore, for the same power level, a DC line requires smaller RoW, cheaper and simpler towers and reduced conductor and insulator costs.

Only two conductors (about two-thirds of the AC line with same current carrying capacity), the absence of skin effects, the less dielectric losses and reduced corona effects are reasons why DC transmission has low costs for operation. The other factors that affect line costs are the costs of compensation and terminal equipment. DC lines do not need reactive power compensation but the terminal equipment costs are more than AC lines because of converters and filters [4].

Figure 2.1 shows that variation of costs of transmission line with distance for AC and DC transmission. DC solution becomes more economical than AC for distance longer than the breakeven distance. The breakeven distance is in a range from 400-700 km in overhead lines. With a cable system, the breakeven distance can vary between 25 and 50 km.
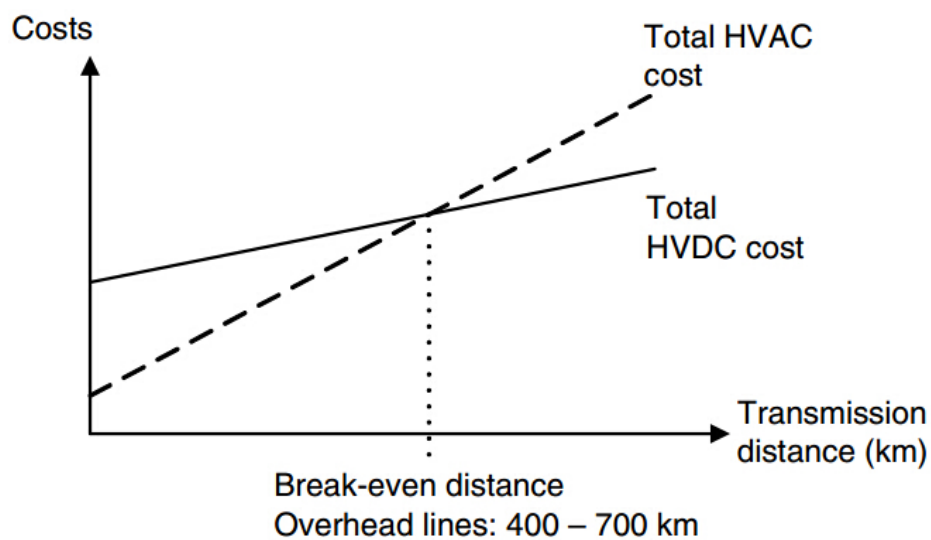
Figure 2.1 Comparison of ac/dc lines [4]

b. Technical performance

The DC solution has some better features than AC solution. DC transmission has more advantages due to the fast controllability of power. The most common arguments favoring HVDC include the following [5-6]:

- Full control over power transmitted
- Fast control to limit fault current in DC lines result in Less expensive breaker and simpler bus-bar arrangements
- The ability to improve transient and dynamic stability in associated AC system.
- The ability to solve problems of AC interconnection-for example, it allows the connection of 50Hz and 60Hz power system.
- Although the converter stations of some types of HVDC need reactive power, it does not need any reactive power to maintain voltage no matter how long the DC transmission line is.

There is another reason for selecting HVDC is the low impact on the surrounding environment.

In fact, DC transmission also have disadvantages which are discussed below:

1. Inability to use transformers to change voltage level
2. The difficulty of breaking DC current.
3. High cost of conversion equipment
4. Generation of harmonics which need AC and DC filters
5. Complexity of control

Over these years, some disadvantages have been overcome and others have been improved at least. HVDC technology gains significant advances.

2.2.2 Types of HVDC

HVDC system requires an electronic converter to convert electrical energy from AC system to DC system or vice versa. There are two types of HVDC converters which are Current Source Converter (CSC) and Voltage Source Converter (VSC).

CSC-HVDC was developed in 1950's from Island Gotland to Swedish Mainland which utilized mercury-arc valve [7]. Its rated capacity was 20 MW. In 1970's the thyristor valve emerges as fundamental switching device. It has been proven highly reliable, and well-studied in CIGRE's collected statistics and sessions. From about 1990, the alternative VSC become economically feasible on account of the availability of new self-commutating high-power switches, such as Gate Turn-Off thyristor (GTO) and Insulated-Gate Bipolar Transistor (IGBT) [8].

Between 1972 and 2015, the installed capacity of all kinds of HVDC has reached over 200,000 MW and continues to grow until today [9]. The largest CSC-HVDC, , which has the highest voltage($\pm$ 1100kV) and power(10000MW), and the longest distance(2600km), is Zhundong-Sichuan project in China. The application of VSC-HVDC is also approaching 1400MW, 500KV. An example is the 1400MW, ±525KV Nordlink that interconnect the grid of Statnett in Norway and TenneT in Germany over a distance of 623km [10-11].

HVDC methods are classified by the power electronic switching devices which convert power from AC to DC [12]:

- CSC–HVDC is the technology that applies line-commutated, current-source converters (LCC-CSC) with thyristor valves (figure 2.2). These converters require a relatively strong synchronous voltage source in order to commutate.
- VSC-HVDC is the technology based on Voltage Source Converter (VSC) with controllable turn-off device (figure 2.3). The current in this technology can both be switched on and off at any time independent of the AC voltage, that is, it creates its own AC voltages in case of blackstart.

VSC technology is distinguished from the more classical LCC-HVDC technology by use of self-commutated semiconductor devices, which have the ability to be turned on and off by gate signal and endow VSC-HVDC transmissions with number of advantages for power system applications. A brief summary of difference between LCC and VSC technology is depicted in Table 2.1 [14].
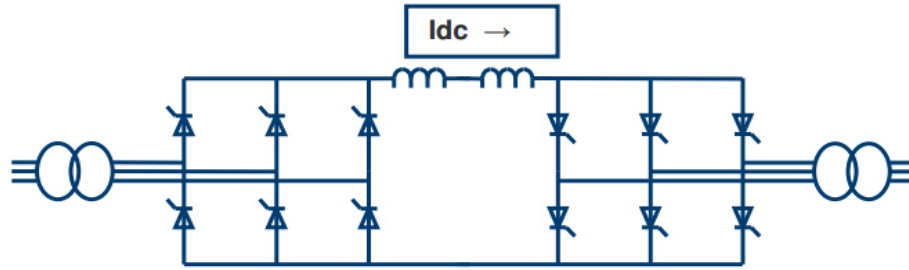
Figure 2.2 HVDC transmission based LCC technology with thristors [13]
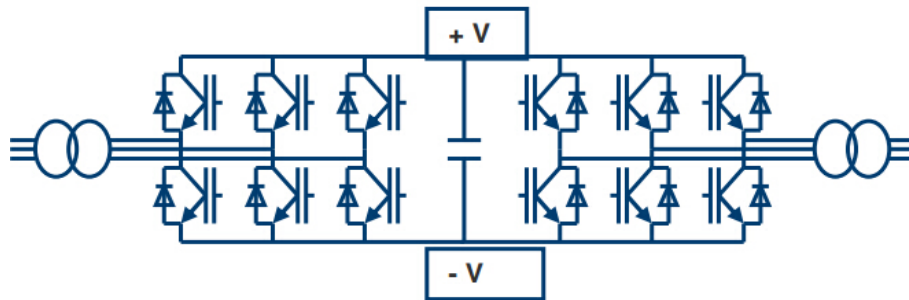
Figure 2.3 HVDC system based on VSC technology with IGBTs [13]

Technology	CSC-HVDC(LCC)	VSC-HVDC
Semiconductor (control)	Thyristor (turn on only)	IGBT (turn on/off)
Power control	Active only	Active/Reactive
AC filter and VAR supply	Require large AC filters for harmonic elimination and VAR supply for power factor correction	Require only a small AC filters for higher harmonics elimination and no VAR supply
Minmum Short-Circuit Ratio	>2	0
economics	Lower capital cost and power losses	Higher capital cost and power losses
Reliability for over 1000MW rating	Yes	No

Table 2.1 Comparison of LCC and VSC [14]

LCC-HVDC so far is the major HVDC solution with advantages of large capacity and lower cost. The reliability and well-established performance of the thyristor means that LCC-HVDC will continue for the foreseeable future to be the main choice for long distance, bulk power transmission. This situation is likely to remain until the

alternative VSC semiconductors achieve similar or better ratings and techno-economic performance than the thyristor [15].

2.2.3 State of the art of LCC-HVDC

In order to meet the growing of power demand, China, Brazil and India began study on the UHVDC transmission technologies at the voltage level of ±800 kV and more recently even up to 1100 kV. Currently, the demand of UHVDC is to transfer 6000-8000 MW over 1000-2000 km at 800 KV. Yunnan–Guangdong HVDC is the first 800 kV UHVDC system in the world which is operated by the China Southern Power Grid in Guangzhou. It was commenced commercial operation in 2009. During the same period, Xiangjiaba-Shanghai HVDC, ±800 kV HVDC Transmission, rated for 6400 MW, to transmit power over a distance of 1935 km, is operated by State Grid Corporation of China (SGCC). The longest HVDC link in the world, with a length 2375km, was built in Brazil named Rio Madeira. ABB was selected by Power Grid Corporation of India to design the world's first multi-terminal 800 kV UHVDC transmission link. The project rated for 6000 MW to transmit power over a distance of around 1728 km to feed power into Agra and New Delhi area [16-19].

In China, due to the inverse distribution between economic development and energy resources, the rational allocation of the energy resource over a large area is necessary. According to the research, the transmission loss will exceed 10% in the case of ±800 kV UHVDC technology. In order to reduce this loss, SGCC proposed to improve the voltage level further, which is ±1100 kV level. The rated power of one of the projects under construction is 10450MW [20]. There will be 30GW electrical power transmitted from Sinkiang to central China through 4 UHVDC lines, one of which is ±1100 kV pilot project, Zhundong-Chengdu project, as shown in figure 2.4. The sending side and the receiving side of Zhundong-Chengdu project are thermal power and hydro power respectively. [21-22].
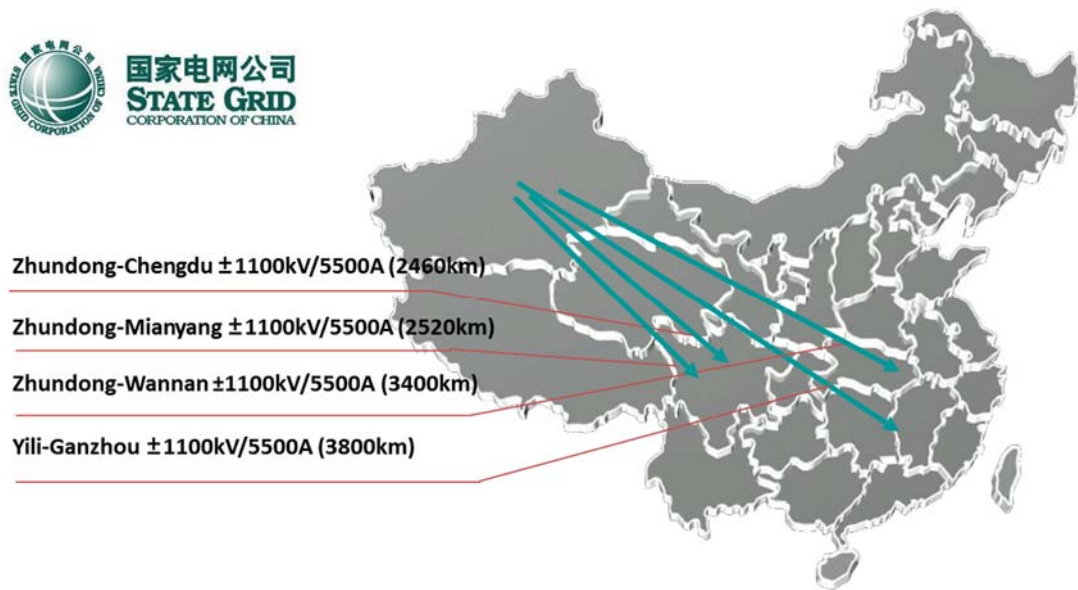
Figure 2.4 ±1100 kV pilot projects [23]

Following the CO2 reduction legislation, all the EU countries are committed to maximise the power output from the low carbon resources such as renewable energy sources to the level of 20% by 2020. In UK, a significant portion of these renewable resources is wind generation which are mainly distributed in the Scotland. In order to transfer the increased renewable energy to the south of UK, the Western HVDC Link (LCC-HVDC link), which comprises converter stations in England and Scotland, linked by a 420 km subsea cable operating at 600 kV was constructed from 2013 [24]. This is the UK's first link to operate at 600 kV direct current, and the longest cable of its type in the world at a 2200 MW continuous capacity. Figure 2.5 shows the planning configuration of Western HVDC Link in UK.
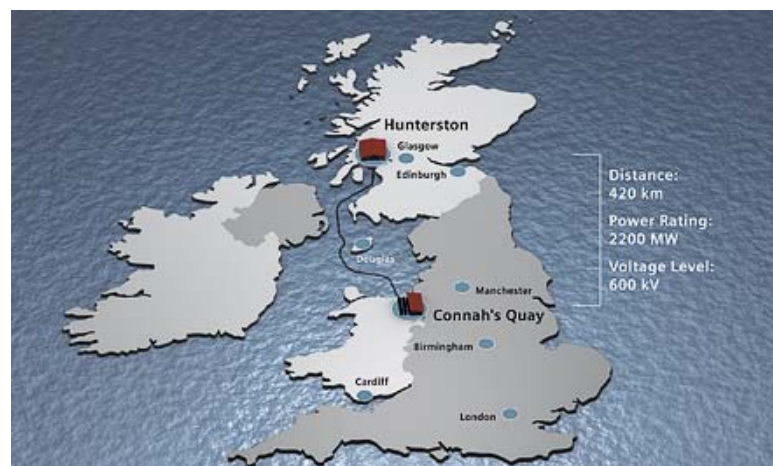
Figure 2.5 Western HVDC Link project [24]

2.3 Coordinated operation of LCC-HVDC and FACTS

The main application of HVDC is the interconnection between AC systems. When a large amount of power has to be transmitted by overhead line or by submarine cable, HVDC links can provide excellent load flow and power damping control. However, LCC-HVDC is usually weak in transient stability control and voltage control for an AC system due to the voltage sensitivity of converter operations. Particularly, with increasing complexity of system conditions, e.g. in weak power systems with enhanced stability requirements, the voltage sensitivity could cause HVDC outage due to commutation failures [26]. The commutation of current from one valve to another has not been completed before the commutating voltage reverses across the ongoing valve, which is defined as commutation failure [27]. This results in a short circuit across the valve group. Under severe conditions, if the recovery after the first commutation failure is not successful, multiple commutation failures occur. This can normally not be tolerated.

To improve LCC-HVDC under weak system conditions, FACTS devices can be applied to operate with the HVDC involved. The improvement of the voltage control can be provided by an additional shunt compensator (such as SVC or STATCOM) and the enhancement of the transient stability can be achieved by using a series compensator (such as TCSC or FSC). Dedicated FACTS devices exist for special applications improving HVDC operations [28].

In future, transmission systems will have to be operated more and more close to their thermal and dynamic stability limits because of economic and environmental reasons resulting in higher loading. The increased loading has impact on power system stability that may cause inter-area oscillations [29]. The impact may get worse when high-power HVDC systems are combined with weak ac systems. Therefore, detailed and careful planning is needed to find an appropriate solution. The coordination of HVDC and FACTS will be the most economical solution fulfilling reliability and operational requirements. To minimize costs and size of the power electronic equipment the approach has to take into account the combined and parallel operation of power electronic equipment. The different controllers in the system have to be coordinated to avoid interaction and to achieve optimal system operation and minimum response times [26].

2.3.1 Example of coordinated operation of HVDC and SVC

In 1995, a major 500 kV transmission system extension has been carried out to increase the power transfer capability between Arizona and California in USA. The extension shown in figure 2.6 includes two main series compensated 500 kV line segments and two equally rated SVCs, supplied by Siemens, at the Adelanto and Marketplace substations. The SVCs are designed mainly to improve the transient stability of the transmission system and to reduce voltage dips on the bus in Adelanto where the inverter station of the 1920 MW HVDC long distance transmission line is connected [30].

The results of the intensive project testing with computer and real-time simulator facilities are shown in figure 2.7 for a fault application at Marketplace 500 kV bus. The influence of the HVDC and AC system can be seen from the DC voltage E_{dc} and Marketplace bus voltage in AC system V_{lt}. Figure 2.7(a) shows that the SVCs are only in voltage control and Figure 2.7(b) shows the results under coordinated voltage and power oscillation damping control [31].
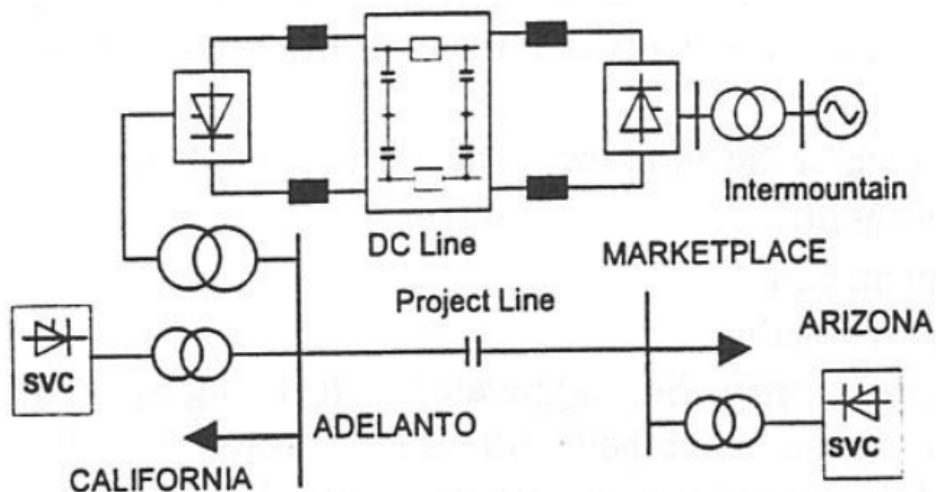
Figure 2.6 Mead-Adelanto AC-DC system [30]
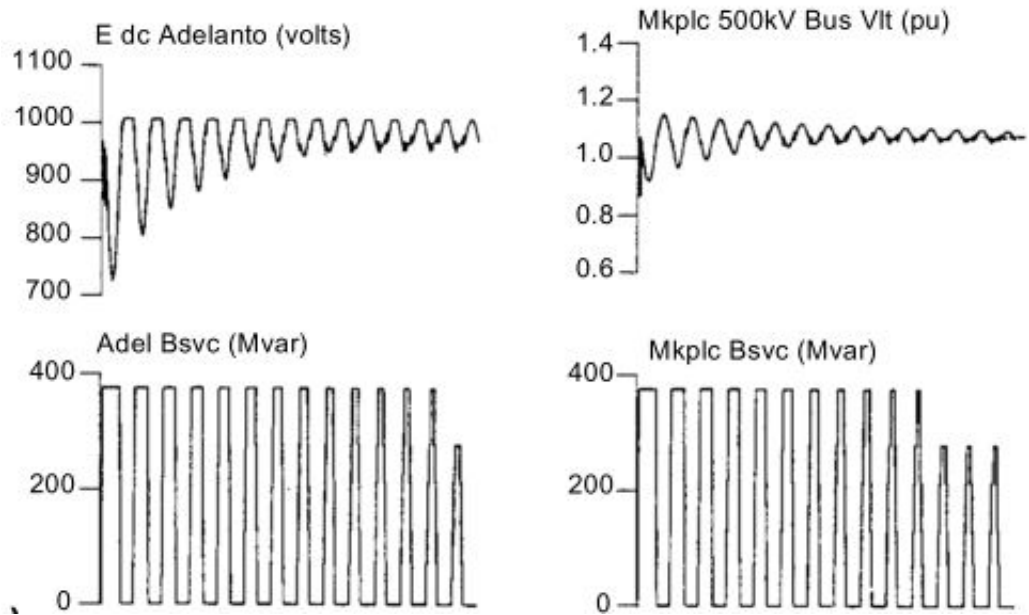
(a) Both SVCs in Voltage Control Mode
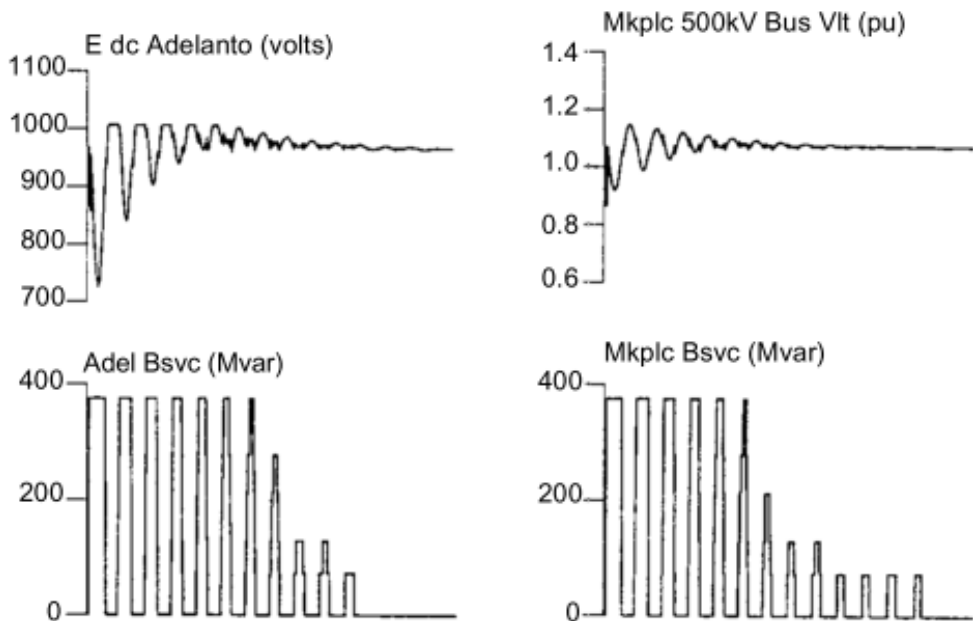
(b) Both SVCs in Coordinated Voltage
& Power Oscillation Damping Control Mode

Figure 2.7 Mead-Adelanto Studies of coordination [31]

A SVC application in combination with HVDC in Germany is presented [32]. As shown in figure 2.8, his project is the first high voltage FACTS controller application in network. The reason for the SVC installation at Siems substation nearby the landing point of the Baltic Cable HVDC were unforeseen RoW restrictions in the neighboring area, where an initially planned new transmission line to the strong 400kV network

for connection of HVDC was denied. Therefore, with the existing 110kV reduced network (the dotted black lines in figure 2.8), only a limited power transfer (350 MW) of the DC link was possible to transmit in 1994 in order to avoid repetitive HVDC commutation failures and voltage problems in the grid.

Finally, the new SVC was installed in 2003, which equipped with a fast coordinated control. The HVDC could fully increase its transmission capacity up to the design rating of 600 MW. In addition to this measure, a new cable (the green line) to the 220 kV grid was installed to increase the system strength with regard to performance improvement of the HVDC control [33].
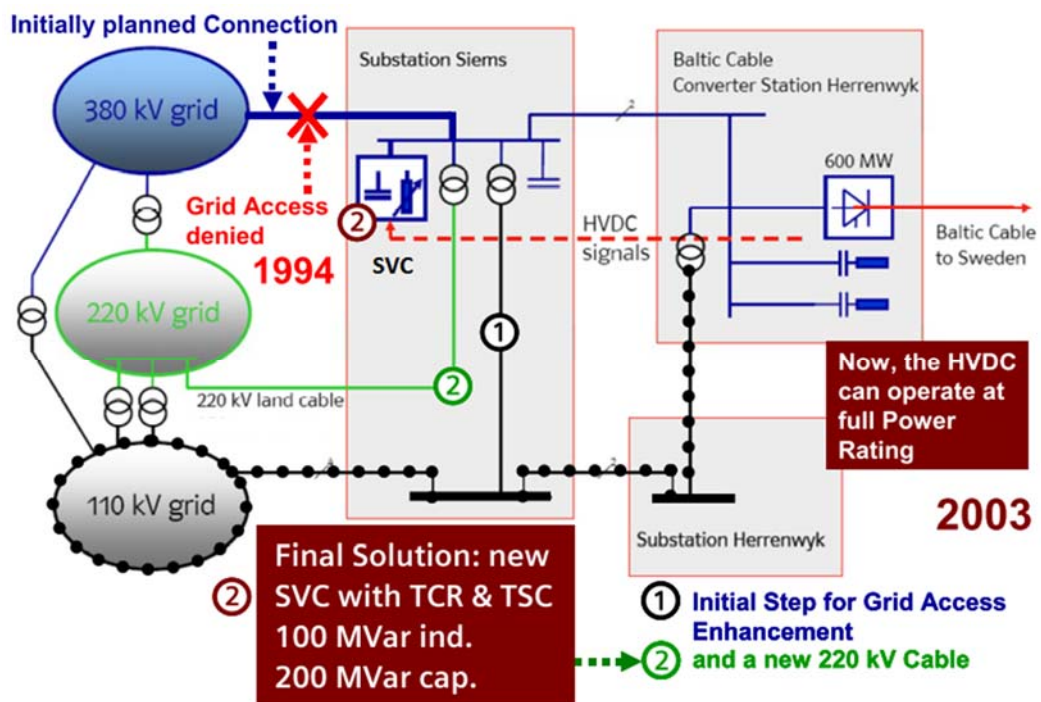
Figure 2.8 The solution for no Right of Way for 400 kV AC Grid Access of Baltic Cable HVDC [33]

2.3.2 Example of coordinated operation of HVDC and TCSC

Figure 2.9 gives an example of a large power system simulation of the Chinese grid [34], in which both FACTS and HVDC have been integrated for AC system interconnection and long distance transmission in a hybrid manner. Due to the long

transmission distances, the network experiences some power oscillations after faults, close to the stability limits. In the recordings in figure 2.10, oscillations are depicted. The first curve shows HVDC transmitting power in constant power mode (curve a). It can be seen that obvious power oscillations occur at post-fault. However, damping control of HVDC Gui-Guang is activated (curve b), the oscillations are damped very effectively. Using series compensation with two TCSCs and two FSCs at Pingguo substation, the stability of the overall system can be further increased (curve c). Thus, without series compensation and without HVDC damping, such a large power system would be unstable in case of fault contingencies [35].
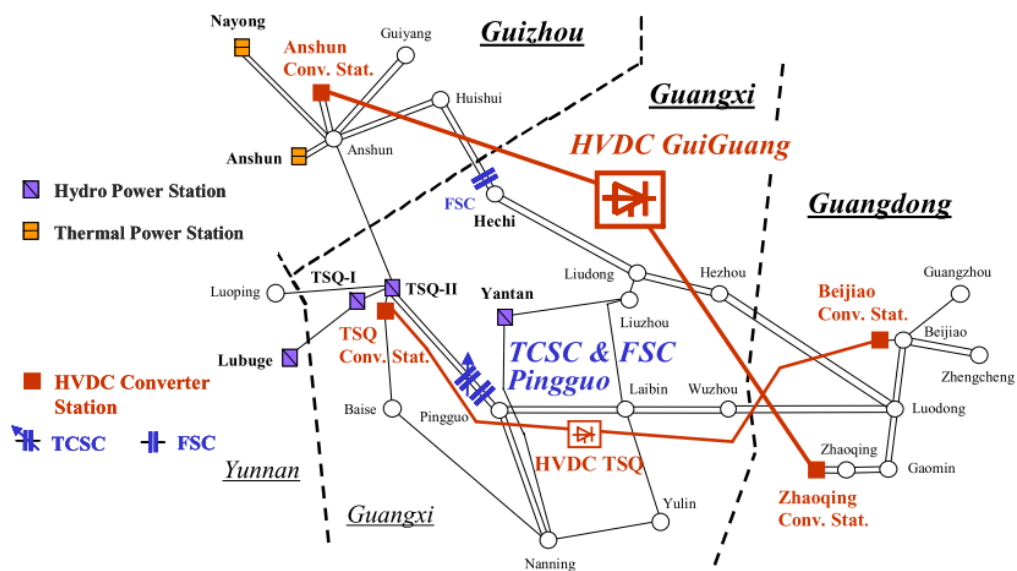
Figure 2.9 Use of HVDC and FACTS in a hybrid System in China [34]
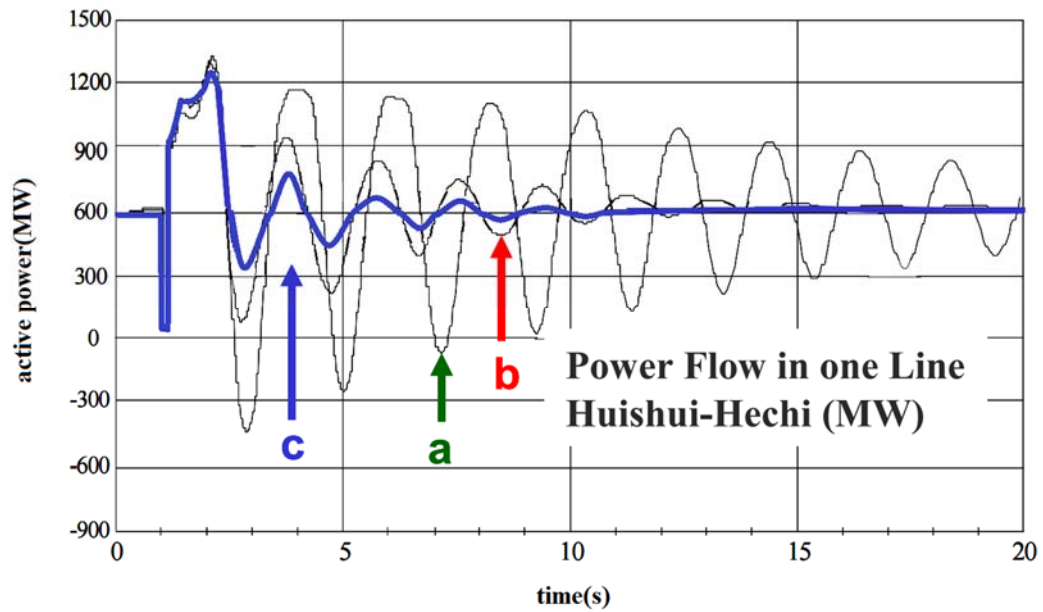
a- without power modulation
b- with power modulation of HVDC control
c- further improvements with Pingguo TCSC

Figure 2.10 Power flows in Huishui-Hechi transmission line [35]

2.3.3 Planning reinforcement of UK

As mentioned in Introduction, facing the increase of wind generations, the GB system operator and owners need to maximize the use of existing transmission lines and operate the transmission lines closer to their thermal limits to avoid constraining some generation plant and also improve the stability limit. A potential solution to provide the higher required transfer capacity to integrate the additional generations is to use some new transmission technologies such as TCSC, SVC and embedded HVDC links which will come into the operation in the GB system between 2013 and 2021 [25]. Figure 2.10 shows the Planning reinforcement (HVDC links, series compensators and Harker SVC) of GB power system. The details and simulations of reinforcement about the Western HVDC Link (LCC-HVDC) and the series compensator (TCSC) will be presented in Chapter 4.

Figure 2.10 Future reinforcements for England and Wales [14]

2.4 Coordinated Control Techniques

The coordination of HVDC link and FACTS devices may result in simultaneous installation of different controllers in power system. The potential interaction exists between multiple controllers. The system stability may be either enhanced or debilitated by the interaction depending upon the chosen controls and placement of FACTS controllers. Therefore, coordinated control techniques, which are utilized to avoid the adverse interaction, need to be investigated. FACTS damping control is superimposed on FACTS normal control functions and so its effectiveness can be hampered by the interaction between FACTS normal control and the damping control function. Based on the relative gain array (RGA) theory, a modified RGA assesses the interactions between FACTS normal control and damping control function [36].

Interactions are divided into several types which are presented in [37]

- Multiple FACTS controllers of a similar type
- Multiple FACTS controllers of a dissimilar type
- Multiple FACTS controllers and HVDC converter controllers

The various interactions occur between the different controllers in power system have been classified into different frequency ranges which include [38]

- 0 Hz for steady state interactions
- 0-3/5 Hz for electro-mechanical oscillations
- 2-15 Hz for small-signal or control oscillations
- 10-50/60 Hz for sub -synchronous resonance (SSR) interaction

Modern coordinated control techniques of HVDC and FACTS controllers are generally classified in three broad categories as sensitivity based methods [39-41], optimization based method [42-43], and artificial intelligence based techniques [44-46].

With the wide application of FACTS in power system, a new major direction of FACTS development is the research of multi-FACTS and FACTS-HVDC coordinated control based on Wide-Area Measurement System (WAMS). Over last decade, the situation was getting better with rapid advancements in WAMS technology which can be applied to form a global measurement and supervision system by integrating the GPS-based phasor measurement units (PMUs), fast communication networks and powerful information technology. In this way, the widely dispersed signals of power systems can be centralized, processed and distributed even in real time, which makes the wide area signal a good alternative for control input [47]. Wide area control systems (WACS) based on modern coordinated methods are responsible of achieving different control objectives through signals and measurements taken of a wide area network. Control objectives can be focused on a large region of the network or part of it. In addition, the control signals could be sent to one or more devices, in the case of multiple control actuators. The WACS are in charge of coordinating control actions for each device [48].

In [49], a robust coordination approach for the controller design of multiple HVDC and FACTS WACS is presented for the aim of stabilizing multiple inter-area oscillation modes in large-scale power systems. A sequential robust design approach, which receives suitable wide-area control signals, is based on the robust control theory and is formulated as a standard problem of multi-objective mixed H_2/H_∞ output-feedback control with regional pole placement constraints. The linear matrix inequality (LMI) theory is applied to solve such a robust control problem. Reference [50] presents a wide-area robust decentralized coordinated control framework for HVDC power system is then put forward, where the upper level wide-area coordinated controller is designed as a dynamic output feedback controller that coordinates the lower level HVDC supplementary controller, PSS and SVC. In [51], an algorithm based on free-weighting matrix approach is proposed for the anti-delay coordinated control among multiple FACTSs, which uses the output feedback signal of wide-area measurement system.

Conclusion

Operation requirements on AC and DC transmission systems will strongly focus on reliability and quality of electrical energy. The HVDC and FACTS techniques have been as an advanced means for improving overall power system performance. To cover a wide range of network configurations and operation conditions, a combination of the HVDC and FACTS devices is often required. The coordination of the HVDC and FACTS devices can provide the necessary operation characteristics, and thus efficiently improve the system dynamic performance, especially under weak and very weak system conditions. In this chapter, a few examples of coordinated operations have been reviewed.

Three main types of methods/techniques for coordinated control between FACTS and HVDC controllers in multi-machine power systems are mentioned in this chapter. An appropriate coordinated control can maximize the control effect, and at the same time, avoid possible adverse interaction among existing devices. In recent years, WAMS-based coordinated control among FACTS controllers is one of the directions of FACTS development because the global measurement is better applied to solve

problem of power system. Several references of WAMS-based coordinated control are addressed in the last section.

Chapter Three: Modelling and control of LCC-HVDC and TCSC

3.1 Introduction

The following sections will outline the modelling and primary control of Line-commutation converters (LCC) based of HVDC transmission networks and TCSC. The benchmark models of HVDC and TCSC have been built and used in the later chapters of this thesis. The modelling and tests are validated by using time domain simulation in Advanced Digital Power System Simulator (ADPSS).

3.2 Introduction to ADPSS

As the complexity of the integrated electric power networks grows, the need for more comprehensive simulation tools rises.

China Electric Power Research Institute took 8 years to research and develop the ADPSS, which achieved both technical breakthrough and theoretical innovation on main technologies such as the real-time simulation of large-scale power system and the electromechanical-electromagnetic transient hybrid simulation. The interior rapid transient change process of HVDC devices can be simulated by electromagnetic simulation. ADPSS integrates all the required functions for power system modelling analysis and simulation. Some of these functions include power flow, fault analysis, transient stability analysis, small signal analysis [52-55].

It also has the capability to integrate new state of art technologies such as power electronic based devices FACTS and wind generation.

The focus of this thesis is on investigating the ability of HVDC link and TCSC to increase the transmission capability and system stability using various control schemes. HVDC links and TCSC models are built and tested in this chapter, which will be implemented throughout the thesis. The concept of a designed controller will be first applied to a test model then to a more realistic system which is the simplified GB power system.

3.3 Modelling and control of LCC-HVDC link

3.3.1 LCC-HVDC link configuration and components

To investigate the characteristics of LCC, the model is built based on CIGRE benchmark which was proposed in 1985 [56]. It is a standard system to provide the reference for HVDC study. The system is shown in Figure 3.1 which is a 500kV, 1000MW HVDC link with 12-pulse converters on both rectifier and inverter sides, connected to a weak ac system (short circuit ratio of 2.5 at a rated frequency of 50 Hz).
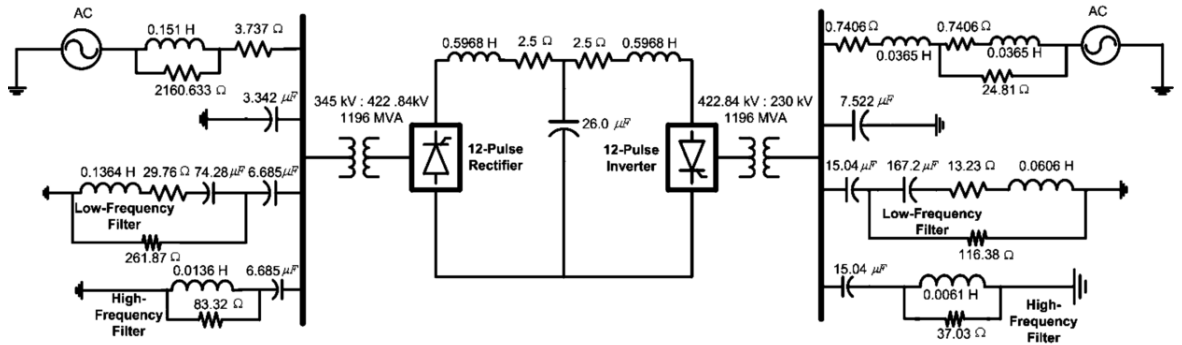
Figure 3.1 Single-line diagram of the CIGRE benchmark HVDC system [57]

The main components of HVDC system include [58]:

Converters: The converter stations are represented by 12-pulse configuration with two six-pulse valves in series. Each six-pulse valves connects to AC bus by a built-in transformer with tap changers which is designed to work with high harmonic current and withstand AC/DC voltage stress.

AC and DC side filters: AC filters are added to absorb the harmonics generated by the converter as well as to supply reactive power to the converter. Some HVDC designs with overhead lines also implement a DC filter.

Smoothing reactors: The DC-side of the converter consists of smoothing reactors, which are mainly required to reduce harmonics at the DC-side, prevent commutation failures and protect valves at post fault. It is usually determined based on DC fault current, communication failure and dynamic stability.

Control system: The rectifier and inverter include various hierarchical control systems which will be explained further in the latter section.

3.3.2 LCC-HVDC link modelling

The equivalent circuit of a CSC-HVDC system is illustrated in Figure 3.2 to show the relationship between DC voltage, (V_d) at the rectifier and inverter side. Also, the principal equations for V_d and DC current, (I_d) at a multi-bridge HVDC links' converter are defined in (3.1) to (3.5). Also, all the parameters are defined in Table 3.1 [6].
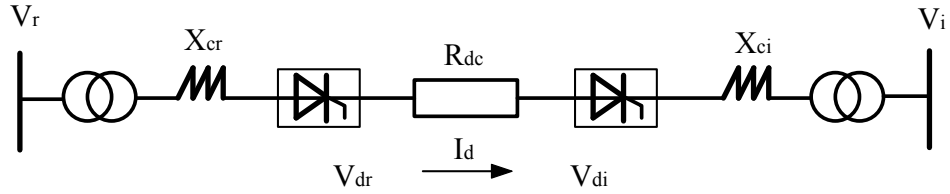
Figure 3.2 Equivalent circuit of the LCC-HVDC system [58]

It is obvious that V_d can be varied by changing the firing angle. As shown in (3.4), the power factor angle is dependent on the firing angle. Hence, the firing angle is typically kept in a low range, around 15°- 20°in order to reduce the reactive power consumption. A sufficient margin is also required to compensate for any AC voltage drop following a disturbance [59]. In addition, AC voltage and the inductance of the converter transformer, (X_{cr}, X_{ci}) can impact the V_d.

As can be seen in (3.3), I_d is proportional to the difference between the converters' voltage. Thus, I_d can be controlled by changing the inverter or rectifier voltage.

$$V_{dr} = B\frac{3\sqrt{2}}{\pi}V_r \cos\alpha - B\frac{3}{\pi}X_{cr}I_d$$

(3.1)

$$V_{di} = B\frac{3\sqrt{2}}{\pi}V_i \cos\gamma - B\frac{3}{\pi}X_{ci}I_d$$

(3.2)

$$I_d = \frac{V_{dr}-V_{di}}{R_{dc}}$$

(3. 3)

$$\cos \varphi \approx \frac{\cos \alpha + \cos \delta}{2} \qquad (3.$$

4)

$$Q_{ac} = P_{ac} \tan \varphi \qquad (3.$$

5)

α	Firing delay angle (start of commutation)	I_d	DC current
δ	Extinction delay angle (end of commutation)	V_r	Line to line AC voltage at inverter side
μ	Commutation overlap angle ($\mu = \delta - \alpha = \beta - \gamma$)	V_i	Line to line AC voltage at rectifier side
β	Ignition advance angle ($\beta = 180 - \alpha$)	φ	Power factor angle
γ	Extinction advance angle ($\gamma = 180 - \delta$)	X_{cr}	Impedance at rectifier side
V_{dr}	DC voltage at inverter side	X_{ci}	Impedance at inverter side
V_{di}	DC voltage at rectifier side	B	Number of series connected 6-pulse bridge

Table 3.1 Definition of the LCC-HVDC link parameters [6]

3.3.3 LCC-HVDC control system

Fast control of current is essential in HVDC. The firing angle (α) is the best controlled quantity due to the rapid response (1~4ms) [60]. α signals to valves are generated from both sides of rectifier and inverter. The voltage and current ultimately can be regulated.

As shown in Figure 3.3, following controllers are used in control scheme [61-62]:

- DC current controller
- DC voltage controller
- Extinction angle controller
- Voltage Dependent Current Order Limiter (VDCOL)

Rectifier control mode

Constant current control (CCC) technique is used in the rectifier control system. However, the rectifier voltage can be increased until the firing angle reaches the

minimum firing angle limit of $\alpha = 2°$. Under this condition, the rectifier moves to constant firing angle mode [62].

Inverter control mode

Inverter control system provides three control modes, including Constant DC voltage control mode, Constant Extinction Angle (CEA) control mode and CCC mode. It is important to ensure the extinction angle big enough to avoid commutation failure. Therefore, the CEA control is a default control at the inverter side. However, this mode of control is less stable during a disturbance or in cases where the DC link is connected to a weak AC network. Therefore, DC voltage control is the main control at the inverter side using a Proportional Integral (PI) feedback control to maintain the voltage at the target level.

If the AC voltage at the rectifier side reduces, the rectifier assists in improving the voltage reduction by reducing its firing angle until it reaches to the firing angle limit. The inverter operates at CCC mode that the inverter current order, (I_{dO-inv}) reduced by a current margin. Hence, there is a 10% margin between the rectifier current order, (I_{dO-rec}) and the I_{dO-inv} at inverter side [62].

Voltage Dependent Current Order Limiter (VDCOL)

The VDCAL control is implemented to reduce the DC current reference when the voltage drops below a predetermined value. This is done to prevent commutation failures from occurring at inverter side. Reducing current reference also decrease the reactive power requirement from AC system which is good for fault recovery [62].
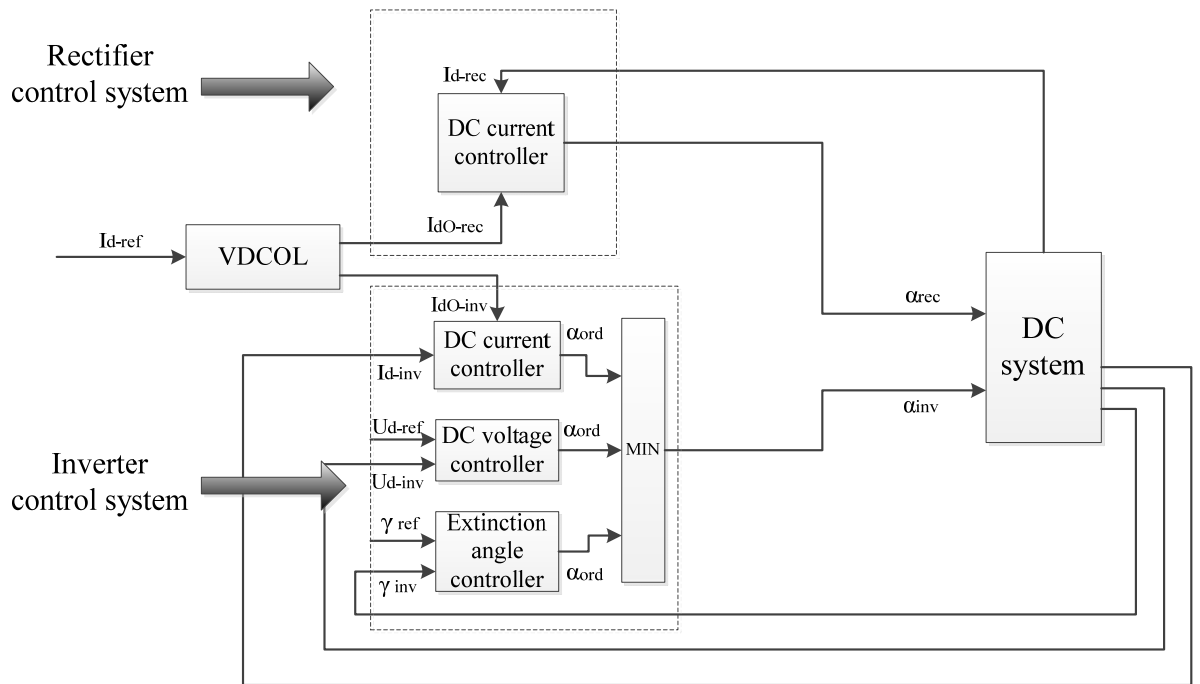
Figure 3.3 LCC-HVDC control system scheme [62]

3.3.4 LCC-HVDC control tests

During stead-state operation, two kinds of controllers are in operation for LCC-HVDC system: DC current controller and extinction angle controller. They all use a PI feedback control to achieve the control targets which need to select the optimum parameters proportional gain (K_p) and integral gain (K_i). In order to verify the default parameters of CIGRE model and study the characteristics of LCC-HVDC control system, the following two tests are recommended [6].

Test 1: 20% step change in DC current reference

To test the performance of the current controller, a negative 0.2 p.u. step change shown in figure 3.4, is applied to its current reference (I_{d-ref}) of 1.0 p.u. at 3s and the step change is affected in 50ms. The response is both stable and well controlled. The DC voltage is also shown, which remains almost constant because it is controlled by the extinction angle controller at the inverter side. The rectifier alpha order signal (α_{rec}) also shows the step change being effected as the average value of alpha is transiently changed from about 19 degrees to about 35 degrees. Eventually the alpha order settles at about 24 degrees for a current at 0.8 p.u.[6].
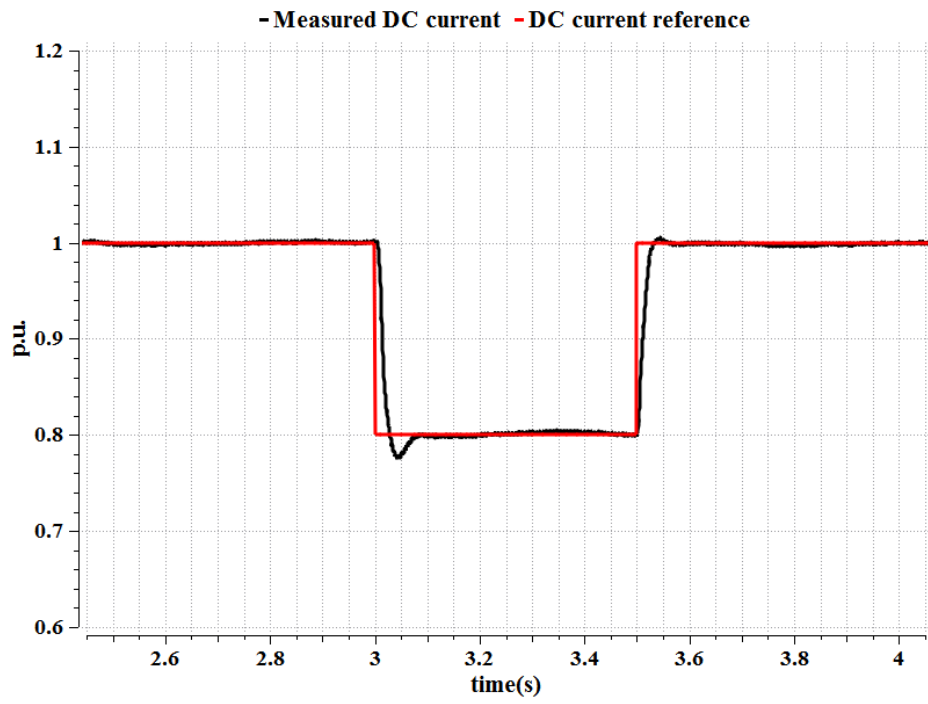
(a)
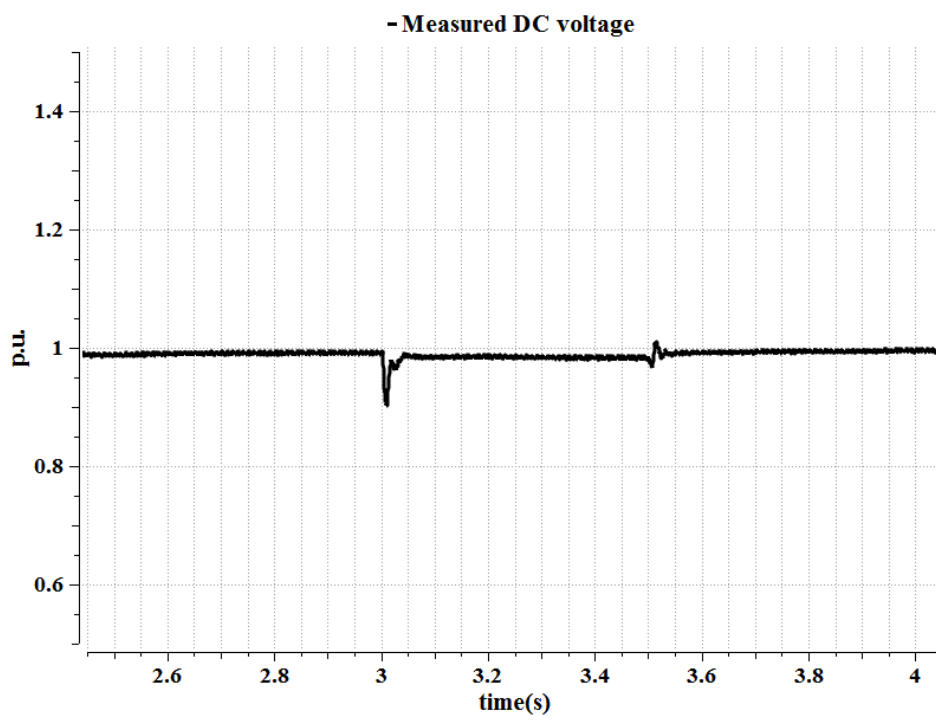
(b)
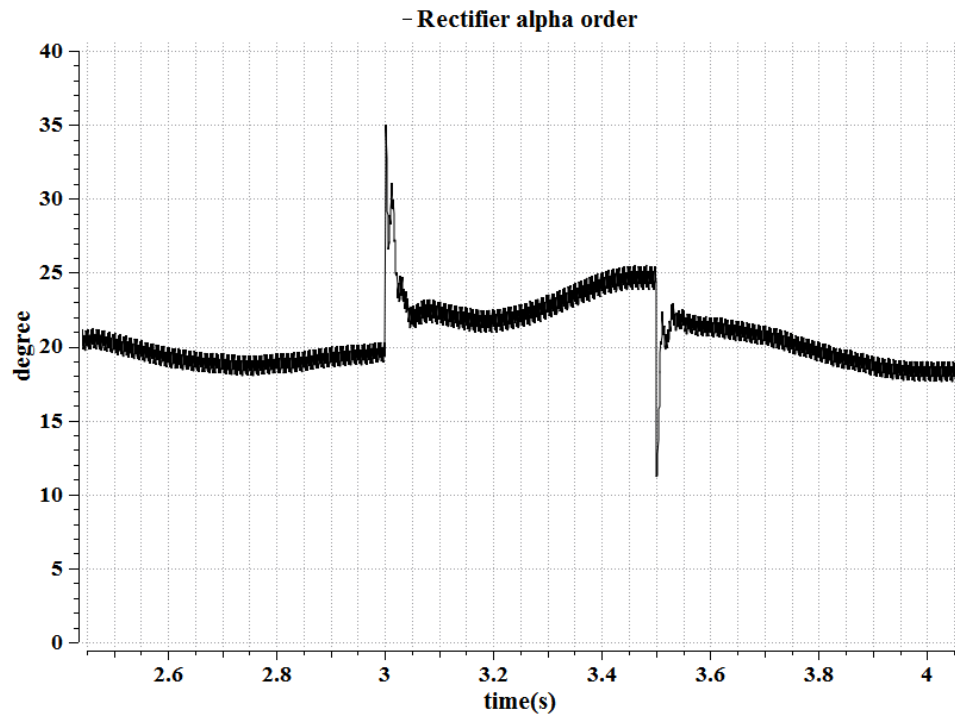
(c)

Figure 3.4 20% step change in DC current reference

Test 2: 2.5° step change in extinction angle reference

In order to test the performance of the extinction angle controller, a 2.5 degrees step change shown in figure 3.5, is applied in the extinction angle reference (γ_{ref}). This increasing step starts at 3s from an original gamma value of 23 degrees to 25.5 degrees and is followed by a decreasing step at 3.5s the response is reasonably stable and well controlled with a response time of 50ms. The DC voltage drops in response to the increase of the gamma value. Consequently, a short-lived transient increase in the DC current is noticed after increasing step of extinction angle [6].
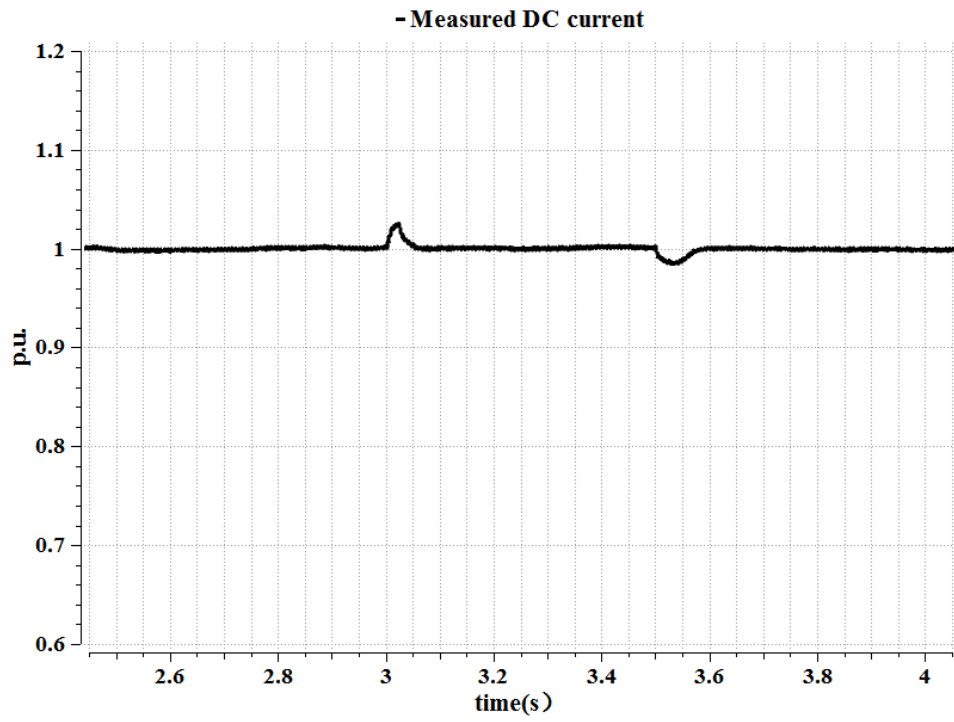
(a)
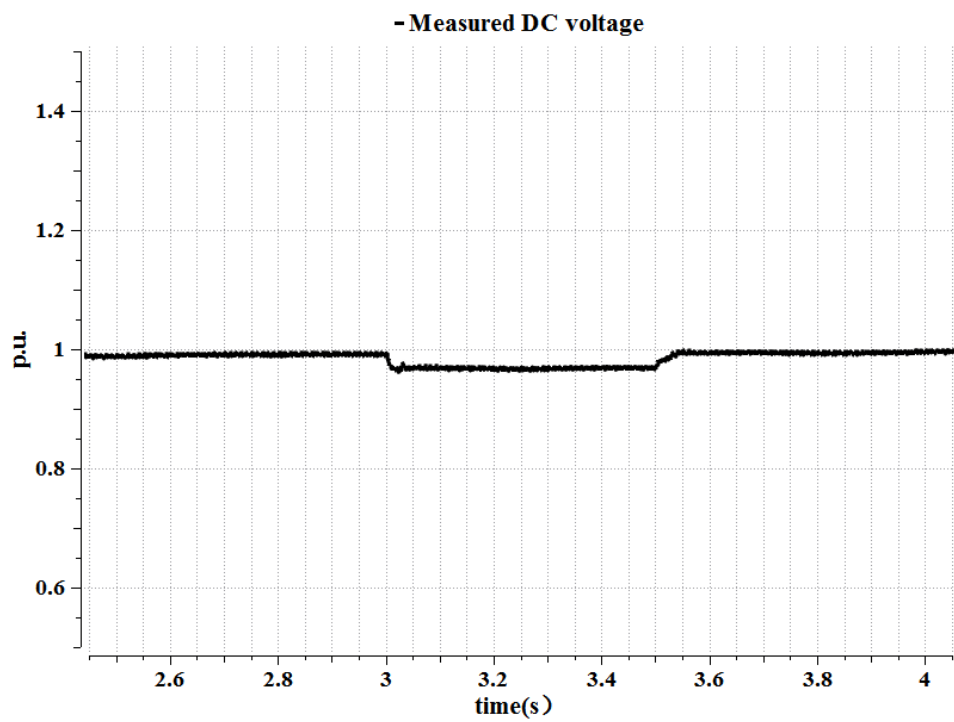
(b)
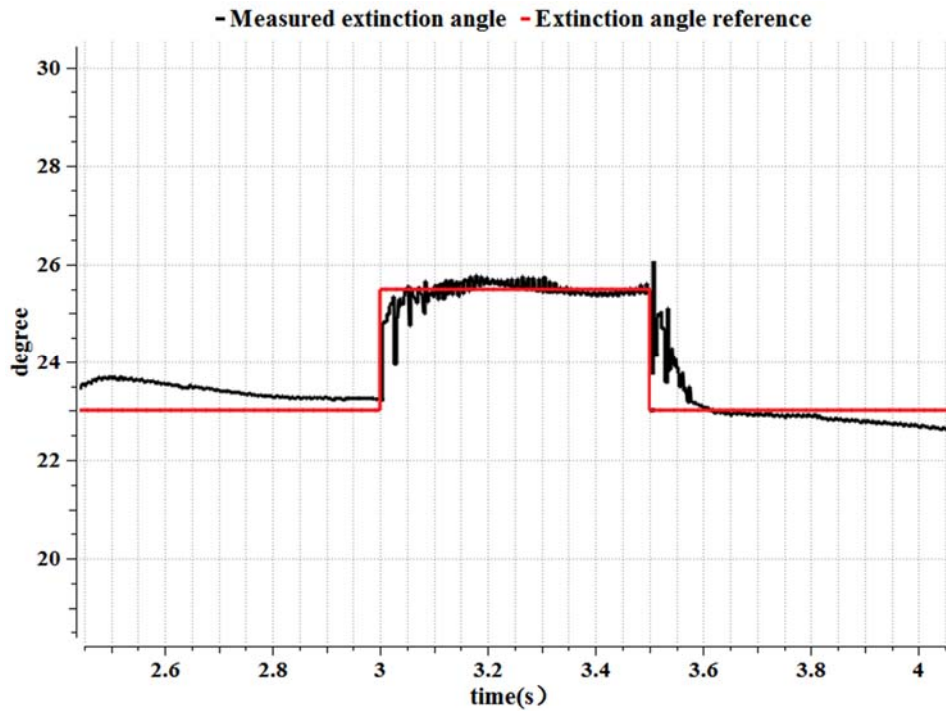
(c)

Figure 3.5 2.5° step change in extinction angle reference

3.4 Modelling and control of TCSC

Series capacitor compensation is widely utilized to increase the power transfer capability because of the fact that capacitor in series with the transmission line increases the inductive impedance. It makes the electrical distance between two AC areas to be shorter [63]:

$$P_1 = \frac{EV}{X} \sin \delta_1$$

(3.6)

$$P_2 = \frac{EV}{X - X_{Cap}} \sin \delta_2$$

(3.7)

Where, E is sending end voltage, V is receiving end voltage, X is reactance of line and δ is phase angle between E and V. Equation (3.7) represents transmission line with series capacitor (X_{Cap}) that more power flow can be transmitted under this condition. For same amount of power transfer, the power angle in the case of series compensated

line is less than uncompensated one which means better angular stability. However, series capacitor compensation may introduce Sub-Synchronous Resonance (SSR) into the system which is caused by adverse interaction between a sub-synchronous mode of torsional vibration on a turbine generator shaft and series compensated network. The characteristic of having a variable reactance makes TCSC has both two capabilities to enhance transient stability and mitigate the SSR [64-66]. SSR problem won't be further studied in this thesis.

3.4.1 Operation principle and model of TCSC

A typical TCSC model, which is similar to SVC, is comprised of a fixed series capacitor C in parallel with a Thyristor-Controlled Reactor (TCR) as shown in figure 3.6. In practice a branch with a Metal Oxide Varistor (MOV) arrester is used to avoid overvoltage. The fundamental frequency equivalent reactance X_{TCSC} of the TCSC model is given by [67]:

$$X_{TCSC} = -X_C + C_1\{2(\pi - \alpha) + \sin[2(\pi - \alpha)]\}$$
$$-C_2 \cos^2(\pi - \alpha)\{k \tan[k(\pi - \alpha)] - \tan(\pi - \alpha)\} \qquad (3.8)$$

Where

$$C_1 = \frac{X_C + X_{LC}}{\pi}$$
(3.9)
$$C_2 = \frac{4X_{LC}^2}{X_L \pi}$$
(3.10)
$$X_{LC} = \frac{X_C X_L}{X_C - X_L}$$
(3.11)
$$k = \frac{\omega_r}{\omega} = \sqrt{\frac{X_C}{X_L}}$$
(3.12)
$$\omega_r = \frac{1}{\sqrt{LC}}$$
(3.13)

Where

$X_L = \omega L$, the reactance of the linear inductor

$X_C = \dfrac{1}{\omega C}$, the reactance of the capacitor bank

X_{TCSC} = Reactance of TCSC

And

α = Firing angle
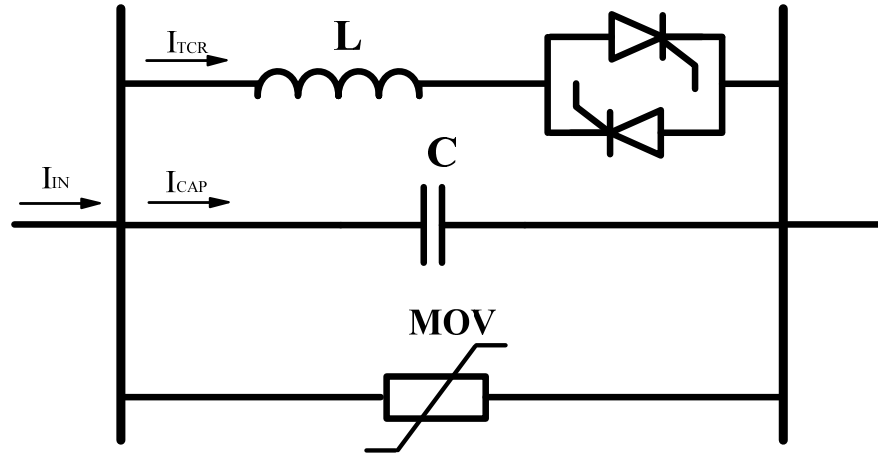
Figure 3.6 Basic TCSC scheme [68]

For a practical TCSC, the compensation capacitance depends on the requirement of power system in which the TCSC is installed. Once the capacitance of compensation capacitor is specified, the minimum capacitance of X_{TCSC} can be determined [69]. To achieve the requirement of power system which will be simulated in the later chapters, the capacitor of the TCSC is taken to be 0.0013F.

Equation (3.8) shows the relation between k and $X_{TCSC}(\alpha)$. The effective reactance $X_{TCSC}(\alpha)$ would be infinity, when,

$$\alpha_{res} = \pi - (2m - 1)\frac{\pi}{2k}; \qquad (m = 1,2, \dots) \tag{3.14}$$

It is clear from equation (3.14), that TCSC may appear multiple resonant points in 90 degrees to 180 degrees of α. Nevertheless, only one resonant point, namely one capacitive range and one inductive range, is allowable. Multiple resonant points will reduce the operating range of the TCSC [70]. Refer to the Kayenta TCSC [71-72], it

is good for operating when $k = \sqrt{\frac{X_C}{X_L}} < 3$ and the only one resonant points is at $\alpha_{res} = 143°$. Thus, the inductance of L can be calculated and taken to be 1.247mH.
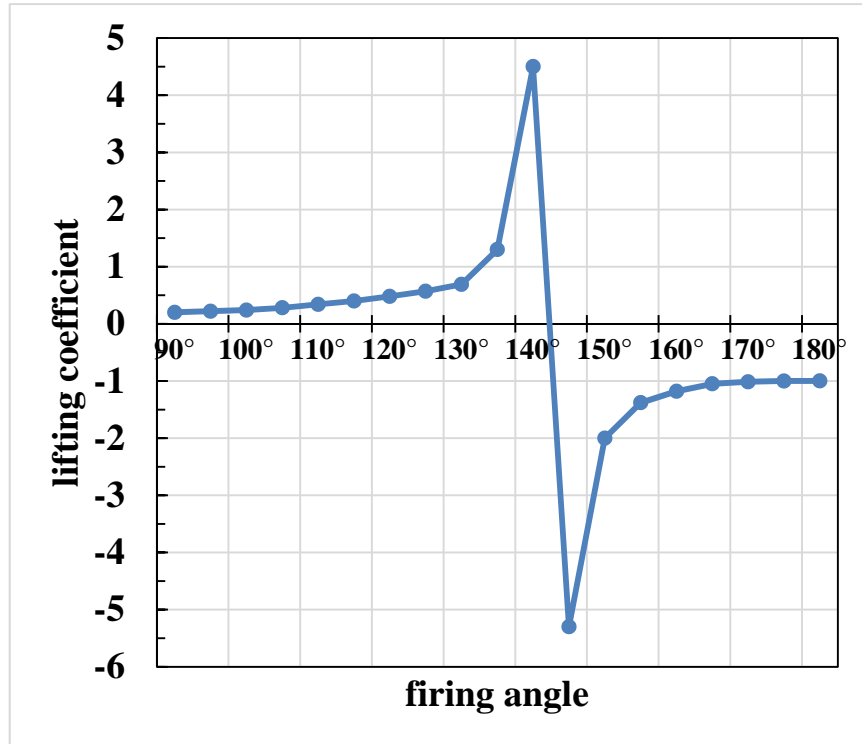
Figure 3.7 Firing angle characteristic of TCSC

Figure 3.7 shows the firing angle characteristics of TCSC for a frequency of 50 Hz. It is drawn between TCSC impedance lifting coefficient and firing angle α. The lifting coefficient is in per units of X_C. The impedance of TCSC can be adjusted in three kinds of modes by controlling α of thyristor [69-70]:

1. Blocking mode ($\alpha=180°$): The thyristor is not triggered and the TCSC is thus reduced to a fixed-series capacitor which capacitance turns to X_C. The power factor of TCSC is leading.

2. Bypassed mode ($\alpha=90°$): The thyristor is triggered continuously and the valve stays conducting all the time. The TCSC behaves like a parallel connection of the capacitor bank with the inductor. The power factor of TCSC is lagging.

3. Vernier mode: The TCSC behaves either as a continuously controllable capacitance ($\alpha_{res} < \alpha < 180°$) or as a continuously controllable inductive reactance ($90° < \alpha < \alpha_{res}$).

The minimum and maximum value of firing angles should be selected in such a way to avoid the TCSC operating in high impedance region (close to resonance) which results in high voltage drop across the TCSC [70]. Thus, the range of firing angle is limited from 145° to 180° when the TCSC is operated as a variable capacitance in practice.

3.4.2 TCSC controller design

As shown in figure 3.8, the TCSC controller consists two main operational blocks, i.e. an internal control and an external control. The function of the external control is to accomplish specified compensation objectives. This kind of control directly relies on measured systems variables to define the reference for the internal control, which is usually the value of the controllable reactance. The function of the internal control is to provide appropriate gate drive signals for thyristors to produce the desired compensating reactance [73].
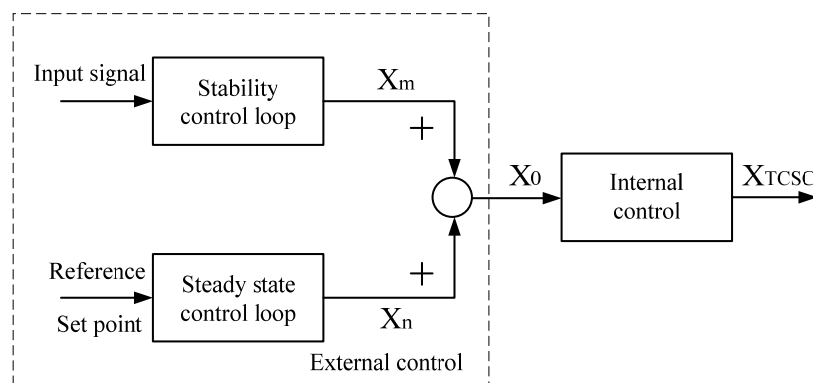
Figure 3.8 Whole control system of TCSC [73]

Internal control

The TCSC's internal control includes a firing pulse generator for thyristors. The α reference signal to pulse generator comes from a linearization curve block. The synchronisation of the thyristor firing controls to the capacitor voltage is achieved indirectly by means of a Phase Locked Loop (PLL) synchronised to the transmission line currents (I_L) [74]. Figure 3.9 illustrate the internal control system.
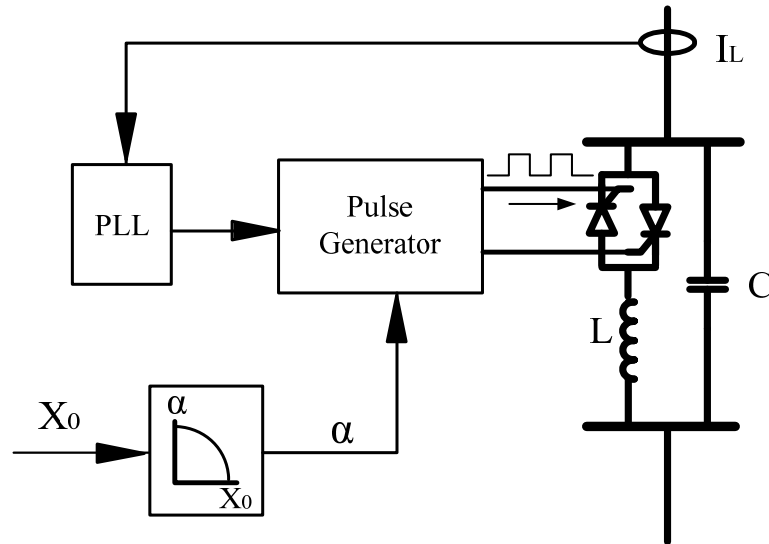
Figure 3.9 Internal controller [74]

External control

The external control may include different control loops depending on the control objectives. As showing in figure 3.8, the principal steady state control of a TCSC is usually a power flow control loop, which is accomplished either automatically with a PI controller or manually through direct operator intervention. Typically, the function of stability control loop is damping controls, which is usually a Power Oscillation Damping (POD) controller [73]. In this study, only steady state control loop is designed in external control system which is a conventional PI controller to regulate the transmitted power.

When TCSC operates in the power control mode as shown in figure 3.10, the conventional PI controller attempts to minimize the power deviation (ΔP) which is difference of reference power (P_{ref}) signal and measured power (P_{meas}) flowing through line and provides the impedance (X_0).
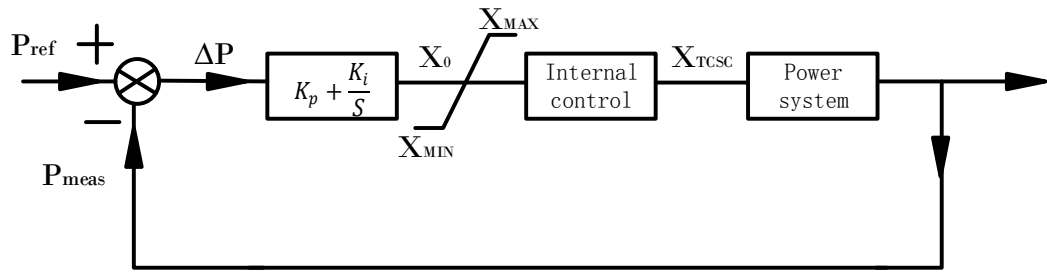
Figure 3.10 Power flow control loop [74]

In order to achieve the appropriate reactance (X_{TCSC}) for regulating the power flow, the internal control is required to control firing angle. Consequently, the regulated X_{TCSC} is applied in power system.

3.4.3 TCSC control test

As the part of LCC-HVDC, the optimum parameters of TCSC controller also should be determined by testing the model. In order to validate the parameters of PI controller offered by [75] and study the characteristic of the TCSC power flow control block, a Single-Machine Infinite-Bus (SMIB) power system installed with the TCSC model, shown in figure 3.11, is built in ADPSS. The SMIB system's generator and transformer models refer to [76] which the base values are $V_{base} = 400\text{kV}$, $S_{base} = 1000\text{MVA}$ and $X_{base} = 160\Omega$.
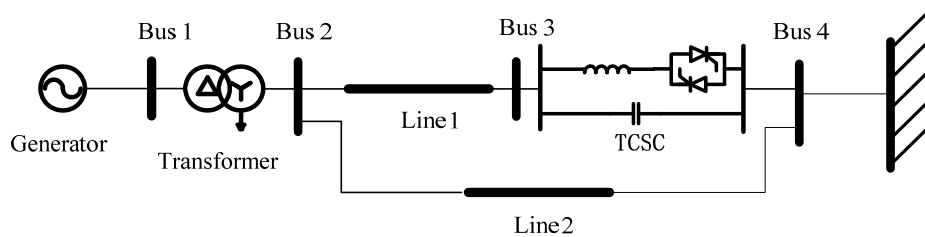
Figure 3.11 SMIB with TCSC [75]

In [75], a heuristic tuning method named Ziegler–Nichols method is introduced to determine the gains of PI controller. As in the method above, the K_i and K_p gains are first set to zero. The proportional gain is increased until it reaches the ultimate gain, K_u, at which the output of the loop starts to oscillate. K_u and the oscillation period P_u are used to set the gains as: $K_p = 0.45K_u$ and $K_i = 1.2K_p/P_u$.

Test 1: power flow controller with gains ($K_p = 6$, $K_i = 60$)

To test the performance of the power flow controller which gains ($K_p = 6$, $K_i = 60$) are estimated by using Ziegler–Nichols method, a step variation of $P_{ref} = [1.1, 1.25, 1.1]$ (p.u.) at time t= [0, 5,10] (s) , shown in figure 3.12, is applied. The results prove that the function of power flow control is actually effective and the parameters of PI controller determined by using introduced method are valid and reasonable. The response of power flow control is stable and well controlled. The firing angle also shows the step change being effected which is changed from about 152 degrees to about 147.5 degrees after the first step. Then, it increases to about 152 degrees again after the second step.
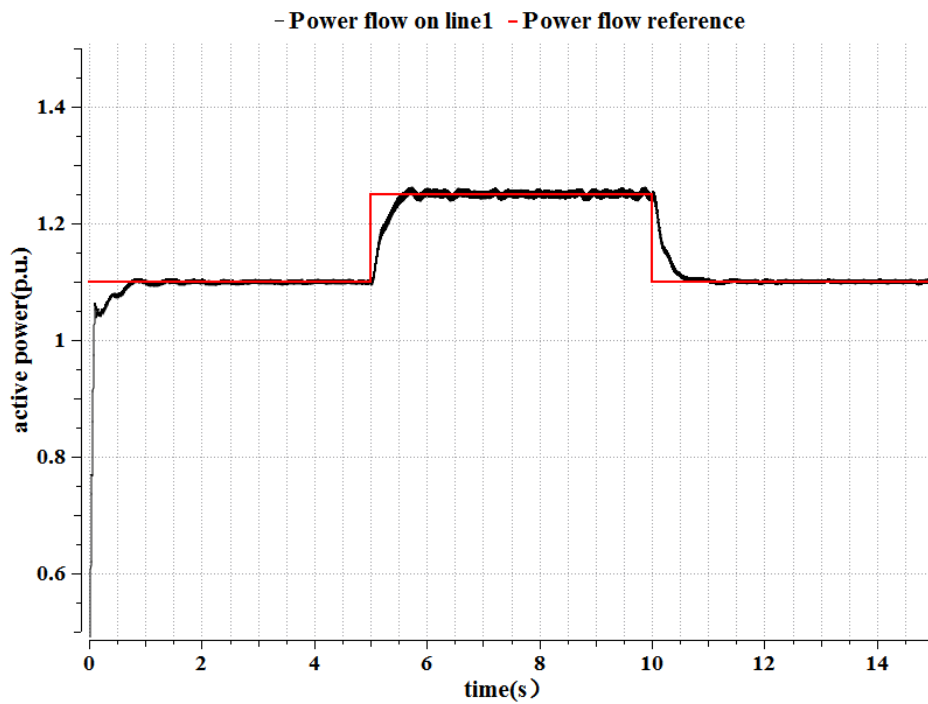
(a)
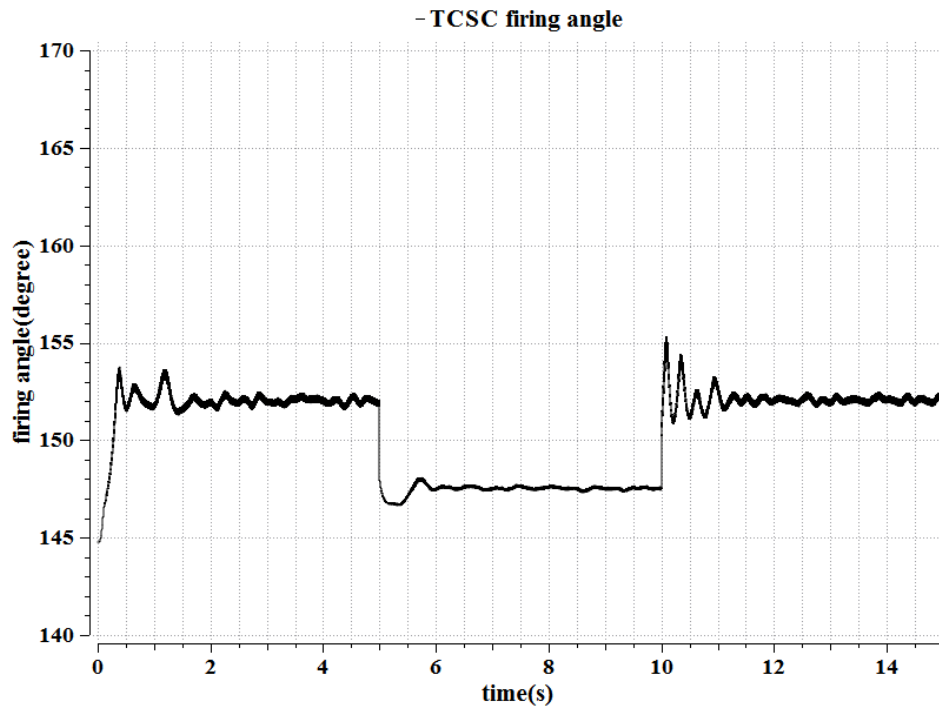
(b)

Figure 3.12 Power flow controller with gains ($K_p = 6$, $K_i = 60$)

Test 2: power flow controller with gains ($K_p = 10$, $K_i = 120$)

To investigate the performance of TCSC power flow control for improper PI parameters design, figure 3.13 shows the test which applies the same step variation as figure 3.12 but with the different gains ($K_p = 10$, $K_i = 120$). Comparing with the result of power flow shown in figure 3.12, the controller has faster response which is affected in 0.2s. However, it also has higher overshoot and the obvious oscillations occur when the P_{ref} rises to 1.25 p.u.. This is not an appropriate setting of PI controller which have worse performance than the test in figure 3.12.
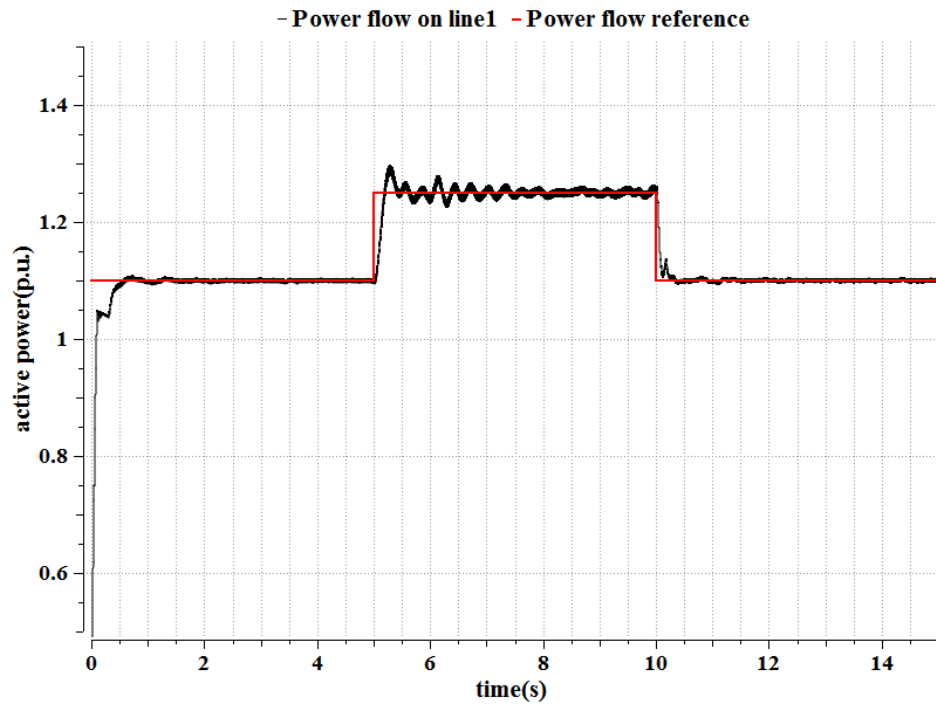
(a)
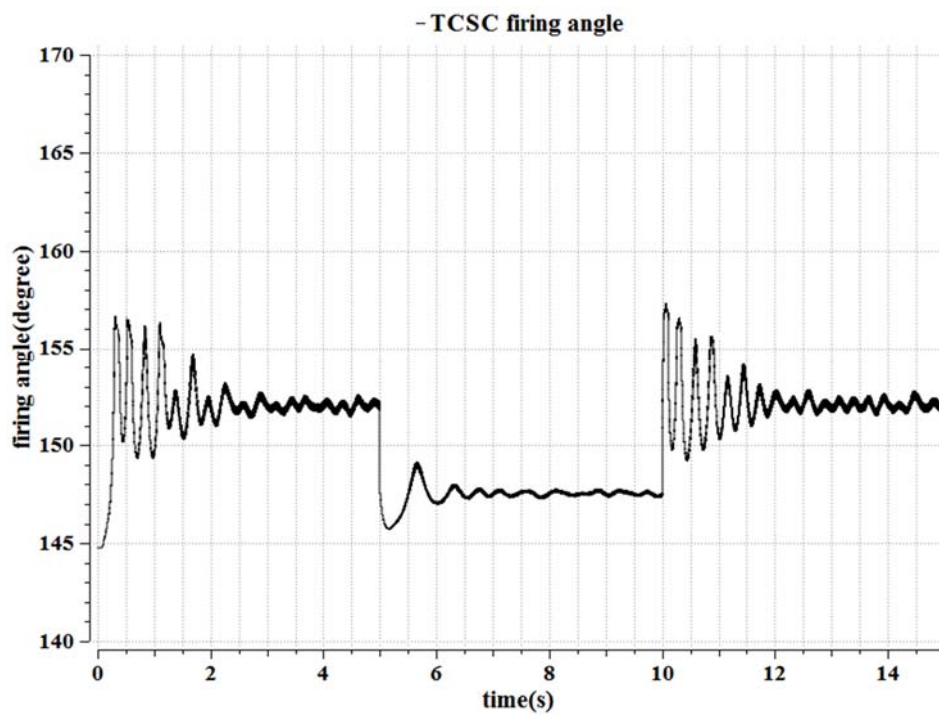
(b)

Figure 3.13 Power flow controller with gains ($K_p = 10$, $K_i = 120$)

Conclusion

In this chapter, following a brief overview of the principles and background theory of the LCC-HVDC link and TCSC, the overall control strategies for the LCC-HVDC link and TCSC are introduced. In addition, both of these two technologies, modelled in ADPSS are presented in this chapter. To study the characteristic of control system and validate the parameters of controllers, the step change tests are illustrated and discussed. In the later chapters, these models are implemented with an objective to study the capability of the HVDC link and TCSC in transient and dynamic stability enhancement for the future GB transmission networks.

Chapter Four: Improving power system dynamics by HVDC and TCSC power flow control

4.1 Introduction

In this chapter, transient stability analysis of the LCC-HVDC link and TCSC in a power system is investigated. The power flow control of HVDC and TCSC is analyzed and corresponding controllers are designed in detail. A three-machine system representing the onshore-reinforced mainland GB system is built in ADPSS software to examine these reinforced new technologies. The dynamic performance of the FACTS device and the HVDC link during serious disturbance are investigated through time-domain simulation. Comparison is also made under different operation schemes.

4.2 Introduction to GB reinforcements

As previously mentioned in chapter 2, following the CO_2 reduction legislation, UK is committed to maximize the power output from low carbon resources such as wind energy source. The main wind generation will be in the Scotland where high levels of wind resources are available. A significant increase of the required power transfer between SPT (Scottish Power Transmission) and NGET (National Grid Electricity Transmission) networks must be achieved. The boundary between SPT and NGET includes two double 400kV AC lines on both eastern and western sides. This boundary, named Anglo Scottish boundary (also known as B6 in figure 4.1) has a current transfer capability of around 2200MW due to stability issues. With the increase in the potential output from wind generation, the crucial problem, which the GB operator and owners encounter, is to maximize the use of existing transmission lines and avoids constraining some generation plants [24-25].

A solution to enhance the power transfer capabilities for integrating the additional generations is to use new transmission technologies such as FACTS devices (e.g. TCSC) and embedded HVDC links. These technologies are going to come into operation in the GB system between 2013 and 2021 as shown in figure 4.1 [25]. Such

power flow controller devices could dynamically change the overall structure and oscillatory behavior of the system and consequently affect the system stability. To cover a wide range of network configurations and operating conditions, a coordinated operation of the HVDC and FACTS devices is often required. This combination can provide the necessary operation characteristics and efficiently improve the system dynamic performance [77-78].
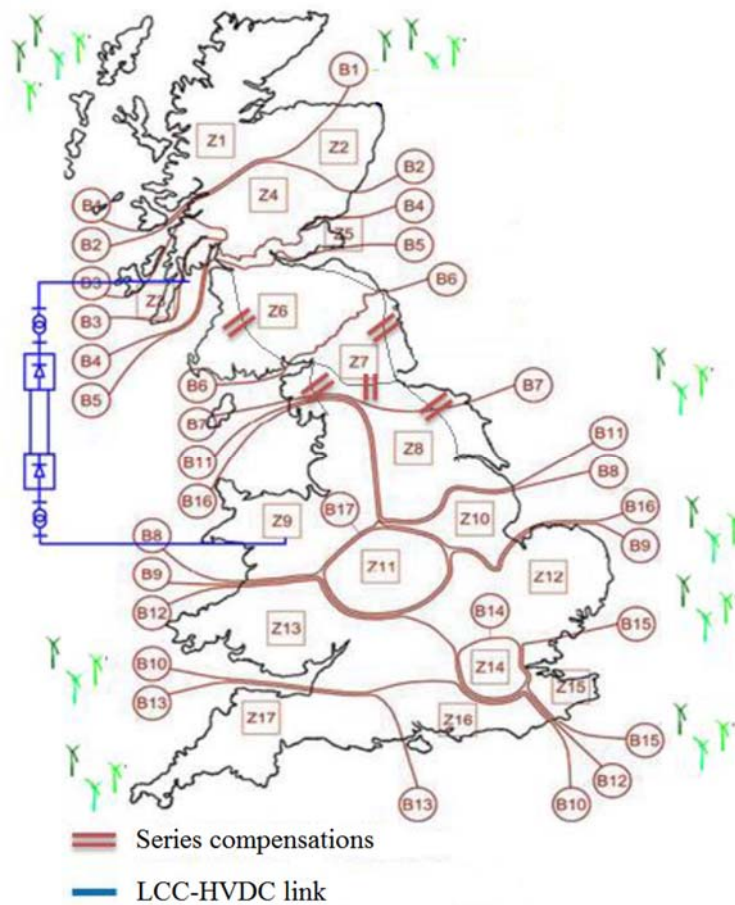
Figure 4.1 Reinforcements for GB power system [25]

4.3 Three-machine power system topology

In order to investigate coordinated operation among FACTS devices and HVDC links, a simplified model to demonstrate the concept of SPT-NGET transmission system introduces in [79-80] is presented in figure 4.2. Three synchronous machines represent three networks in different area, which a HVDC link is applied to transfer power generated by windfarm. A TCSC is installed between bus 7 and bus 8 which can

control the power flow on line 1 while also affects the power flow on line 2. All parameters are given in Appendix.

The most mature technology of the HVDC transmission is LCC type. The reliability and well-established performance of the thyristor means that LCC-HVDC will continue to be the main choice for the foreseeable construction plan. The HVDC model in the 3-machine system is built based on the CIGRE benchmark which was proposed in Chapter 3. Reactive compensation and filter are also provided on both sides. The rectifier station is connected to Northern Scotland area and the inverter is on England-Wales side. Under steady-state, the transferring power flow of each transmission line is also shown in figure 4.2.
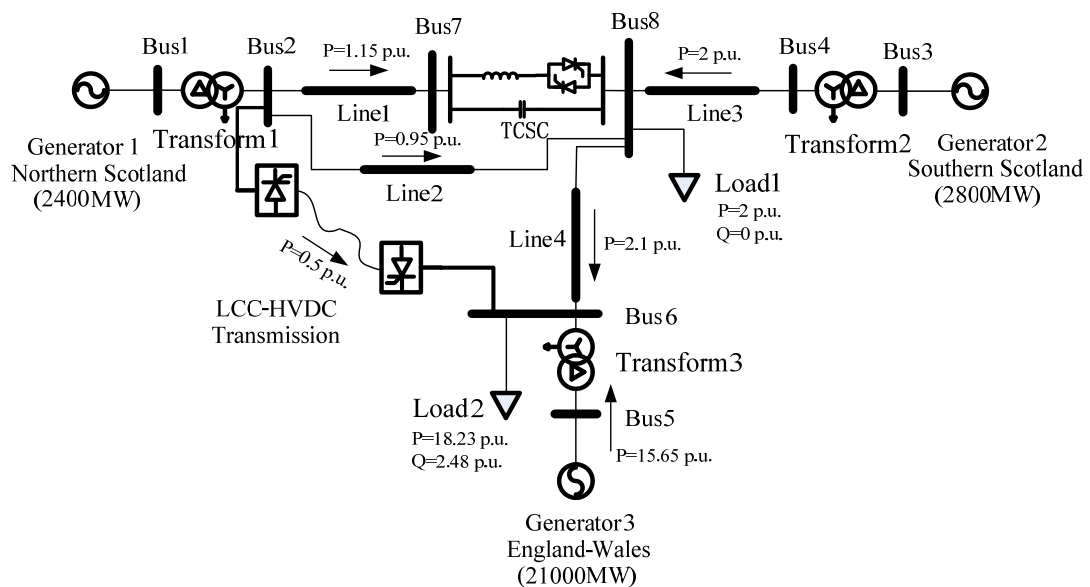
Figure 4.2 3-machine system topology

4.4 The power flow control scheme of TCSC and LCC-HVDC

a. TCSC

At this stage of the research, a simple and conventional stability control scheme is implemented for TCSC using a PI controller to control the power flow on transmission line. As presented in previous chapter, the PI controller of TCSC has examined and determined the parameters. The TCSC controller also consists of a limiter which is used to improve the controller response to large deviation of input signal [74]. The range of firing angle acting on thyristors in this model is limited from 172° to 145°

where the TCSC is only operated as a variable capacitance. As shown in figure 4.3, the lifting coefficient can be adjusted from 1.01 to 5.3 which is the multiple of capacitance of fixed capacitor. In the 3-machine model, the inductance of line 1 is 0.0509 H. Therefore, to meet real-world engineering conditions, the fixed capacitor is taken 0.0013F ($X_C = 0.02$p.u.) such that the compensation level of the line with TCSC can be adjusted from about 20% to higher level [81]. The active power flow ($P_{Line\ 1}$) through the line containing TCSC is taken as the control variable. It is compared with the reference value of active power flow (P_{ref}), and then the error is fed into the PI controller. The output of the PI block is the expected impedance (X_0) inputted to the internal controller. The corresponding firing angle α is achieved in the internal control to regulate the actual impedance (X_{TCSC}) of TCSC.
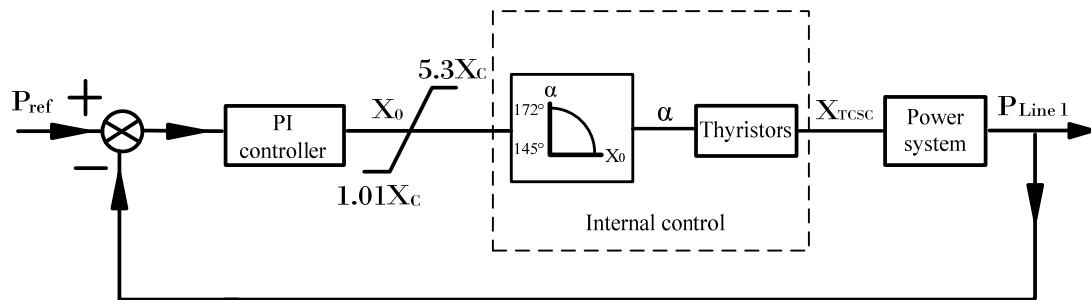
Figure 4.3 Block diagram of whole TCSC power flow control

b. LCC-HVDC

In general condition, the Extinction Angle Control is the default control at the inverter side to maintain the DC voltage and the Constant Current Control is the default control at rectifier side to regulate the DC current. As presented in figure 4.4, the DC power controller is a hierarchy master level control which in fact provides the current reference ($I_{ref-pow}$) to the DC current controller at the rectifier side (VDCOL does not regulate the DC current reference in normal operation, so $I_{ref-pow}$=I_{d0-rec}.). The figure 4.5 shows that the DC power controller also facilitates the power control by continuously calculating the DC current reference related to the measured DC voltage (U_{d-meas}) [62]. It is a closed-loop control to regulate the DC power flow that outputs

the more accurate and appropriate DC current reference than when the Mode select module selects the constant current value.
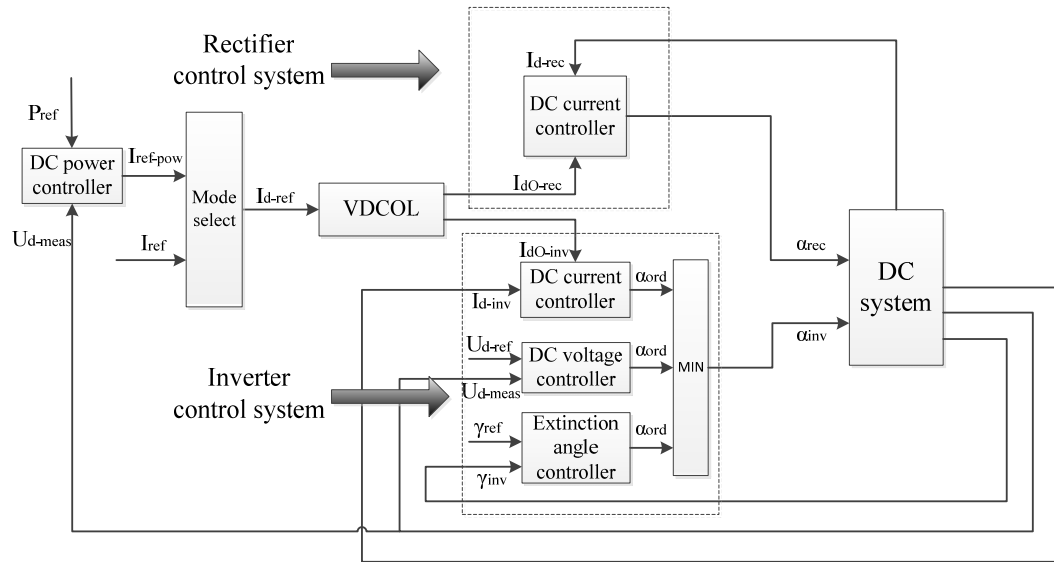
Figure 4.4 LCC-HVDC control system scheme with DC power controller
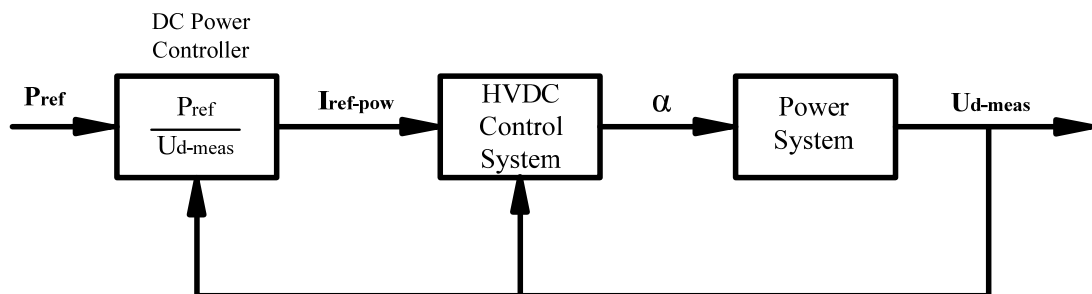
Figure 4.5 Block diagram of LCC-HVDC power control

4.5 Simulation and test results

Three cases under similar conditions were tested and compared to study the combined operation of TCSC and HVDC. Results of simulation is represented by per unit value except firing angle. The voltage base value of AC and DC power system are 400kV and 500kV and the apparent power base of whole system is 1000MVA. A three-phase short circuit fault at time t=7s and cleared at t=7.1s is set at bus 8 for transient stability analysis.

Case 1: In this case study no power control of LCC-HVDC link nor TCSC was applied. The constant DC current reference ($I_{ref} = 0.5\ p.u.$) is directly inputted to DC current controller which the power flow of HVDC (P_{DC}) is maintained at 0.5 p.u. in steady-state due to keeping DC voltage at 1 p.u. by EAC. TCSC is operated under constant impedance control that the compensation level of line 1 is 30%. In this compensation level, the line with TCSC transmits 1.15 p.u. of active power. This case will be used as a benchmark for comparison. The simulation results of the first case in figure 4.6 indicate that power oscillations last longer time than other cases. As shown in figure 4.6(c), the DC power has two obvious oscillations after fault, one has the same frequency as the power flow through line 1 and the other one is a low frequency oscillation about 0.3 Hz.

Case 2: The TCSC is series connected in line 1 and the power flow control is applied to maintain the power flow through line 1 as case 1 (P_{ref} =1.15 p.u.). HVDC link still operated without the power flow control. As it was expected and demonstrated by the simulation results, TCSC controller minimize the power oscillation by regulating the power flow on line 1 at the post-fault. The figure 34(a) indicates that the active power on line 1 return to steady-state at 11.5s which is faster than case1. According to the curve of firing angle in figure 34(b), the impedance of TCSC (X_{TCSC}) is controlled to adjust compensation level of line 1 between 20% and 75%. As shown in figure 4.6(c), there is no obvious improvement to damp the oscillation of DC power flow. It means that applying power flow control of TCSC has little effect on DC power transfer.

Case 3: based on case 2, DC power control mode is selected to maintain the constant power flow on HVDC link that P_{ref} is set 0.5 p.u.. As shown in figure 4.6(c), the better performance of power flow on DC transmission line is achieved which the low frequency oscillation is damped. Figure 4.6(d) indicates the difference of rectifier firing angle between with and without DC power control to regulate the DC current.

DC power controller provides better tracking ability and stronger robustness to regulate the power flow than just inputting a constant I_{ref} signal. However, applying DC power control also has little effect on AC power transfer that the performance of post-fault oscillation on line 1 is almost the same as case 2. Although the coordinated operation of TCSC and HVDC in this power system has no significant interaction no matter adverse or favorable, they increase the power transfer capability and improve the transient stability respectively.
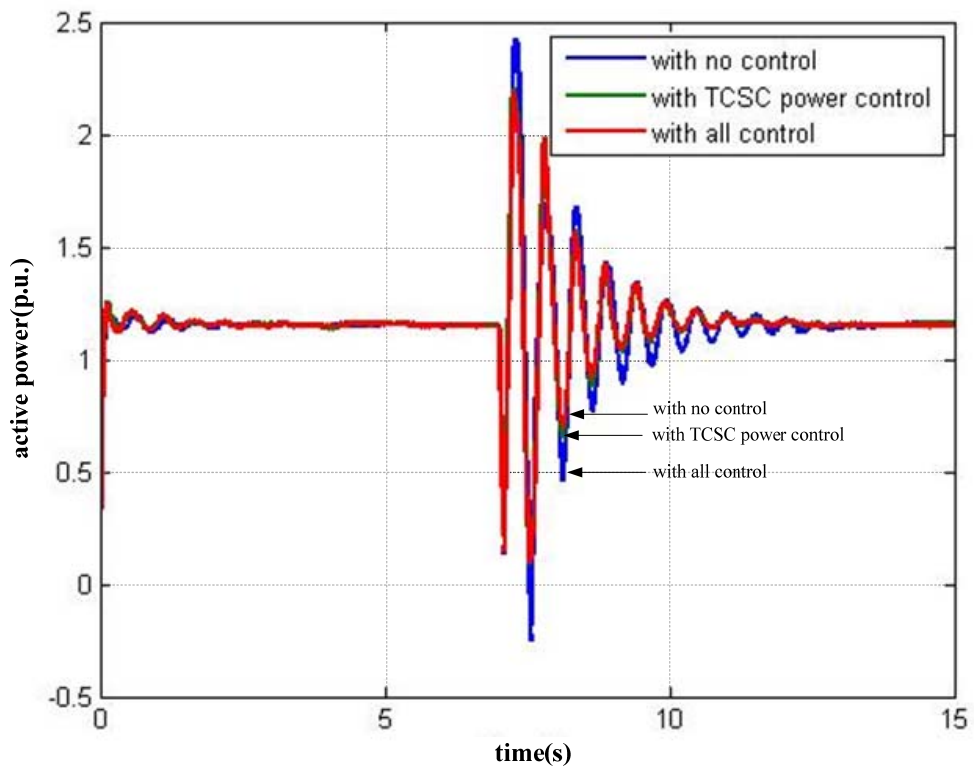
(a) Active power flow on line 1
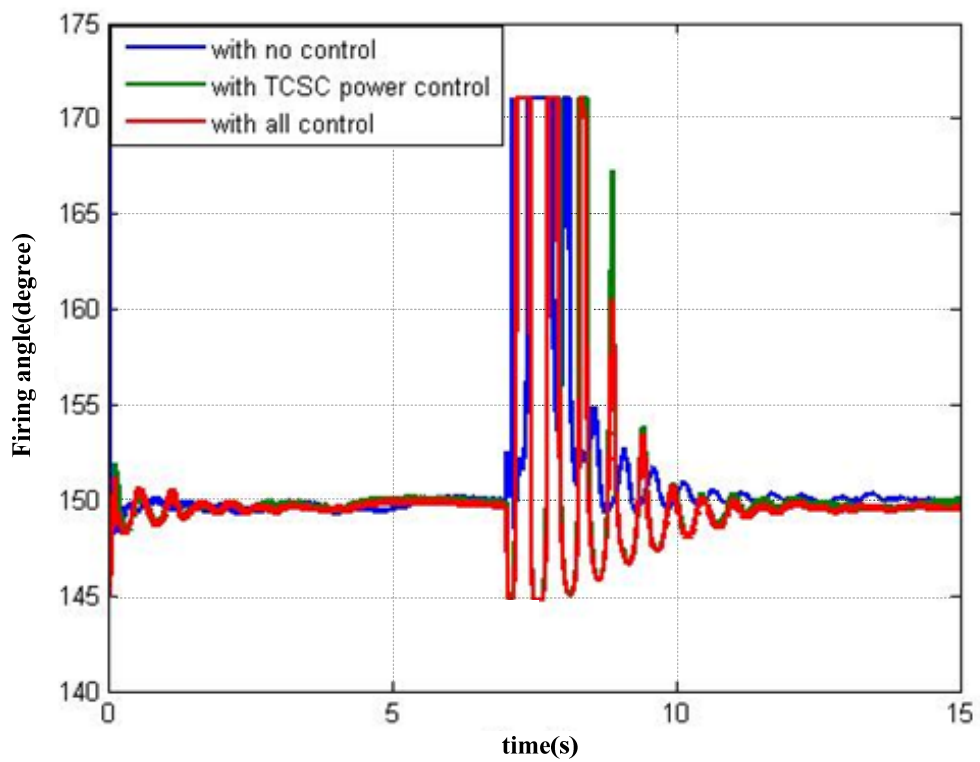
(b) Firing angle of TCSC
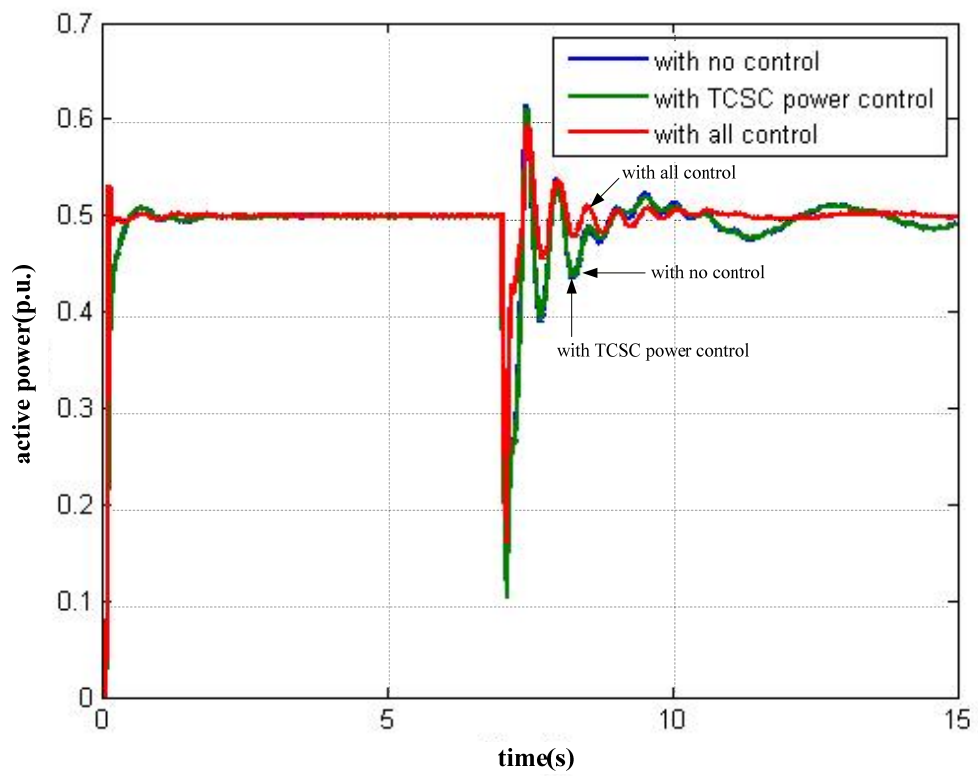
(c) Power flow on LCC-HVDC link
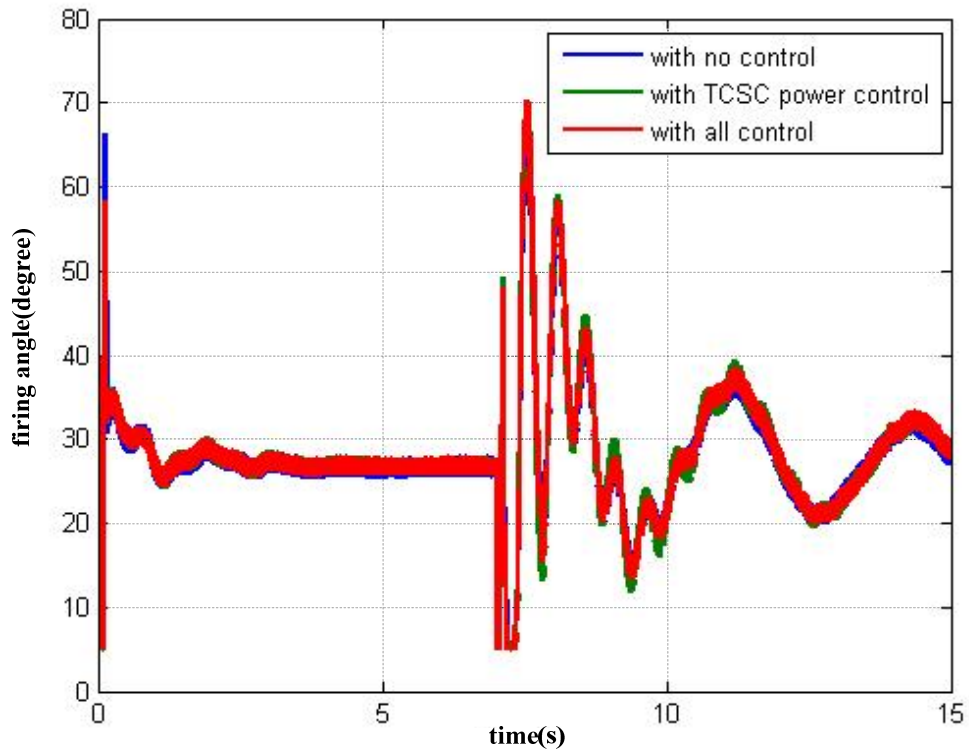
(d) Firing angle of HVDC rectifier converter

Figure 4.6 Results of simulation

Conclusion

In this chapter, the methods of power flow control of TCSC and LCC-HVDC link are presented and the reason for requirement of GB power system to these two new technologies is also introduced. The test system, a simplified model to demonstrate the concept of SPT-NGET transmission system, is built in ADPSS software. The simulation results illustrate the effect on the transient stability of power system by applying power flow control of TCSC and LCC-HVDC link. In the cases of this chapter, there is no obvious interaction between two power flow control devices. Even so, coordinated control is still needed to achieve the optimal results for power system. A coordinated controller will be designed in next chapter.

Chapter Five: Coordinated control for dispatching power flow among TCSC and HVDC

5.1 Introduction

The power flow control by using TCSC and HVDC is presented in previous chapter. These two kind of thyristor-controlled devices shown good performance of stabilizing the transient disturbance at the post-fault. Power flow on transmission lines in congested areas often approaches or goes beyond limit in order to satisfy the increased electric power trades and consumption. Therefore, reliable supply and secure operation are urgent problems due to higher risks of fault lines. HVDC and FACTS devices have abilities to influence power flow and voltages to solve these problems depending on different types of devices. This is where the new technology of HVDC and FACTS offers an important opportunity [82].

Breaking the transmission line is a common protection after faults in power system which may cause frequency deviation between areas and power swing. Power flow on other transmission lines may reach physical or thermal limit [83]. TCSC and HVDC can solve this problem by optimal power flow controlling. Coordinated operation is needed to determine the new set-points of two power flow controllers at post-fault. This chapter will present a coordinated control using TCSC and LCC-HVDC link which are embedded within two areas to keep the total power transfer constant. It can be achieved by a supervisory controller based on Dispatcher Power Flow (DPF) [84]. This high-level controller is designed in this chapter to dispatch the power flow that can maintain the total power flow as pre-fault.

5.2 Power swing

Power swing is caused by large disturbances in a power system. Severe system disturbances could cause large separation of generator rotor angles, large swings of power flows, large fluctuations of voltages and currents, and eventual loss of synchronism between groups of generators or between neighboring utility systems.

Thus, preventing or reducing power swing can improve the transient stability of power system [85].

The electrical power, P_e , transferred from a generator to another area is given by the equation:

$$P_e = \frac{E_g E_l}{X} \sin \delta$$

(5.1)

Which has already presented in chapter 3 (equation 3.1). The swing equation of the machine is [86]:

$$P_a = P_m - P_e = \frac{H}{\pi f} \frac{d^2 \delta}{dt^2} + D \frac{d\delta}{dt} \qquad (5.2)$$

Where:

P_m is Mechanical Turbine Power of the generating unit;

P_e is Electromagnetic Power output of the generating unit;

P_a is Accelerating Power;

H is the inertia constant in seconds;

D is the rotor damping constant in s^2.

The mechanical power, P_m, is provided by the turbine and the average mechanical power must be equal to the average electrical power, neglecting losses. When a system disturbance occurs, the value of one or more parameters of the electrical power equation may be affected. Changing the reactance between two areas (X), the receiving end voltage (E_l) or combination of these two parameters leads to difference in electrical power. For example, a short circuit results in reduction of the load voltage, a breaker opening results in increase of the reactance. When the electrical power does not equal to mechanical power, the rotor will accelerate or decelerate, which leads to deviation from synchronous speed. It results in oscillations in rotor angle and power flow swing. Therefore, maintaining the total transferred power on the boundary of two areas could reduce the power swing effectively.

5.3 Coordinated controller design

In order to dispatch the optimal power flow on transmission lines after fault, a high-level controller is designed in this section to modify the pre-fault set-point of power flow controllers' input signals ($P_{tcsc-ref}$ and $P_{hvdc-ref}$). The objective of the coordinated control is to stabilize the power system by minimizing the power swing of the either side against each other or reducing the frequency deviation. The frequency deviation between areas is in proportion to the deviation of real power flows transmitted on the boundary. The coordinated controller is able to minimize the power swing and frequency deviation by keeping the total transferred power flow as constant as pre-fault.

As shown in figure 5.1, the simulated power system is quite similar to the system simulated in previous chapter of which parameters are presented in Appendix. The power is desired to transmit 2.6 p.u. in total from Northern Scotland area to the loads in England & Wales area. At the steady state condition before fault, the set-points of TCSC and LCC-HVDC link power flow controllers are set to 1.1 p.u. and 0.5 p.u. respectively. A new AC transmission line (line 3) is added on the boundary because TCSC cannot control power flow without any parallel transmission line when a transmission line is open or tripped. The machine generates constant cumulative power that couldn't change no matter what impedance value of TCSC on a single line [87].

The coordinated controller to re-dispatch the power flow on transmission lines is shown as figure 5.2. The active power flow on line 3 (P_{line3}) can be measured by Wide-Area Measurement System (WAMS) in practical application. With the global information measured by WAMS as an input signal, these FACTS-based controllers can obtain rapid advancement in power systems [88-89]. When the breaker on line 3 is open, at immediate post-fault, the loss of that line will be picked up and shared by lines under coordinated control. The dispatched proportion of picked-up active power (ΔP) is determined by parameter K. As an exact value of K is selected, the re-dispatch function can be applied. Two new set-points ($P_{tcsc-ref}$ and $P_{hvdc-ref}$), provided by coordinated controller, are sent to the power flow controller of TCSC and HVDC when

the active power flow on line 3 has changed. The appropriate dispatched proportion can be studied and implemented thanks to more than one power flow control devices in the power system. Optimum coordinated power control will improve the stability performance of whole network.

However, not every setting of parameter K can perform a good coordinated operation of TCSC and HVDC. Either TCSC or HVDC has its specific operation range. If the value of K is set to make the set-point of power flow controller to exceed the limit, the ideal control effect will not be achieved. The limit of TCSC refer to the minimum and maximum value of firing angles which is selected in such a way as to avoid the TCSC operating in high impedance region (at resonance). Working beyond the limit may result in high voltage drop across the TCSC. As presented in previous chapter, the range of firing angle of the simulate model is limited from 145 degrees to 172 degrees that can vary the lifting coefficient of impedance from 1.01 to 5.3.

The way to control the power flow of LCC-HVDC link is to control the DC current of DC link. As presented in previous chapter, rectifier control system controls the DC current and the DC voltage is maintained by inverter control system in general condition. In order to increase the DC current to transmit more power, the voltage at rectifier side should be increased by reducing α of rectifier. The practical alpha-min limit ($\alpha_{min} = 5°$) is required for the valves to have a forward-bias voltage before turning on. Thus, a limiter is set in the LCC-HVDC model to prevent little firing angle and the corresponding maximum transmission power is 1 p.u. (1000WM).
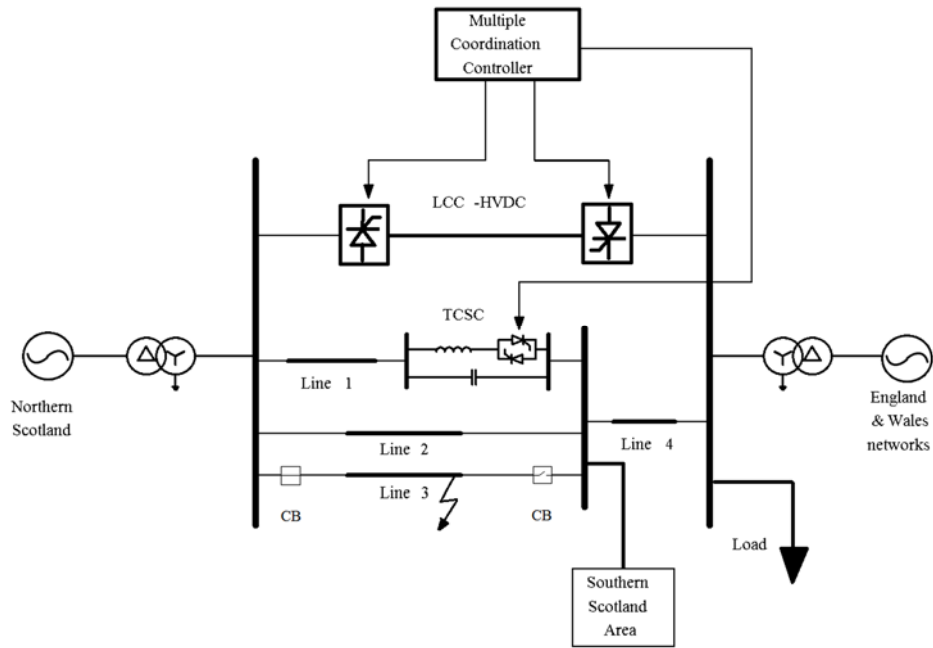
Figure 5.2 Power system with coordinated controller
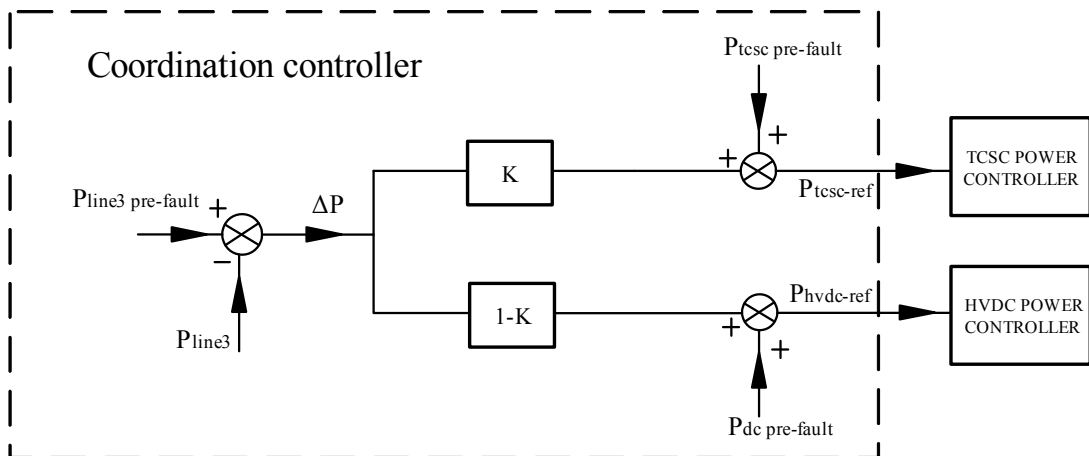
Figure 5.3 Block diagram of coordinated controller

5.4 Simulation studies

A three-phase fault is set on line 3 at t=6s and the breaker trips to isolate the faulty circuit immediately. In order to focus on how the coordinated controller keeps the total power flow as constant as pre-fault, the time to detect the fault and communicate is neglected. Six cases applying different parameter K were simulated and compared to study the optimum dispatched control after fault. Results is represented by per unit value except TCSC firing angle and the difference of the rotor angles (rotor angle of

Northern Scotland minus rotor angle of England & Wales network). The voltage base value (AC 500kV and DC 400kV) and apparent power base value (1000MVA) are similar to previous chapter model. The summary of the simulation results is tabulated in table 5.1.

Case 1 (no coordinated control): the coordinated control is not applied in this case study. The set-points of power flow controllers of TCSC and HVDC link remain at 1.1 p.u. and 0.5 p.u.. As shown in figure 5.4 (a), (b), (c), only HVDC link regulated power flow at 0.5 p.u., TCSC does not work at post-fault because the limitation of firing angle was reached at 172 degrees (figure 5.4 (d)) which means it operates as a fixed series compensator. The power oscillations after the fault occurrence is much higher than other cases with coordinated control.

Case 2 (K=0): the coordinated control is applied in this case and the picked-up power flow is desired to be fully dispatched to HVDC link. However, the maximum power transferred of HVDC is 1 p.u. so that the rest power flow is picked up by AC transmission lines. Table 5.1 indicates that there is 0.75 p.u transferred power flow lost from line 3. The rest active power (0.75-0.5=0.25 p.u.) cannot be picked up completely by line 2 as predicted because of the same reason as case 1. The lowest compensation level of line with TCSC is reached but the stability of system is still better than case 1 due to less transmission requirement of AC transmission lines.

Case 3,4,5,6 (K=0.3,0.5,0.75,1): In this four cases, TCSC and HVDC link both operate in controllable range. As it is expected and demonstrated by simulation results, the power oscillation at post-fault is damped and suppressed with coordinated control. Especially the system quickly returns to steady-state at 7.5s when the parameter K is set 0.3 and 0.5. As the values of K are reduced in this four cases, the differences of rotor angles (figure 5.4 (e)) become smaller and easier to restore to stability because of falling transmission demand of AC transmission system. Figure 5.4 (b) reveals that HVDC link has very robust transmission reliability in controllable range no matter how much active power it transfers. Therefore, the lost power flow should be dispatched to HVDC link as much as possible and the rest of it is picked up by TCSC that makes the rotor angles difference keep lower. The low and stable rotor angles difference means that generators haven't lost synchronism and the rotor angle stability

of power system is good. By comparison, the coordinated control of case 3 (*K*=0.3) have best performance under this condition.
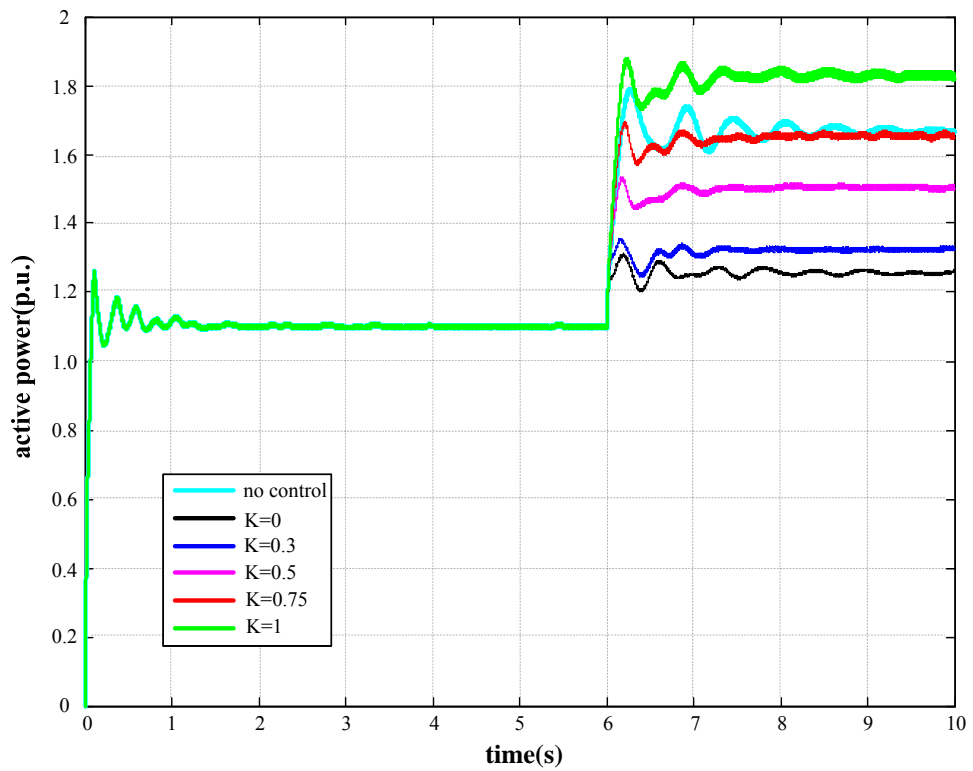
(a) Power flow on line 1(TCSC)
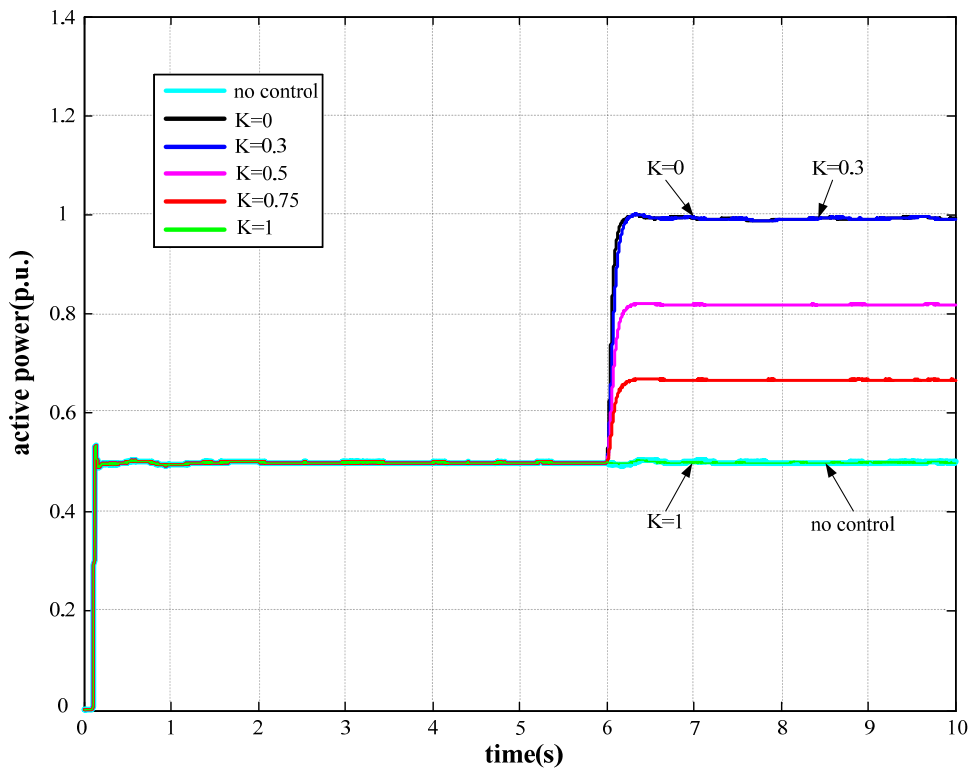
(b) Power flow on LCC-HVDC link
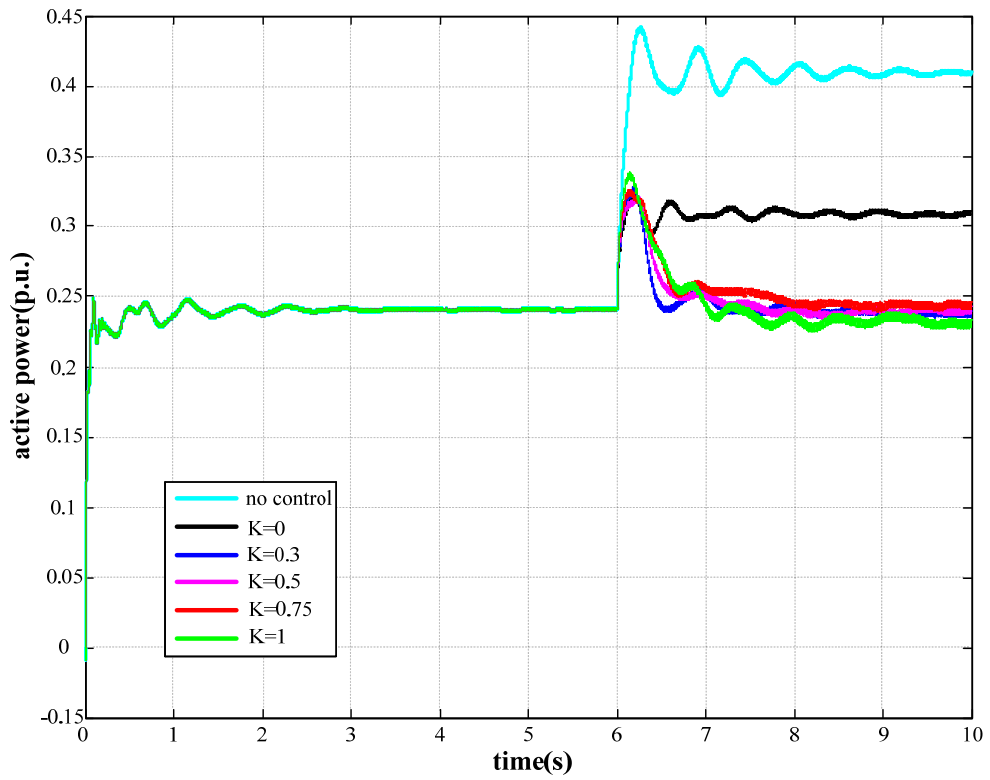
(c) Power flow on line 2
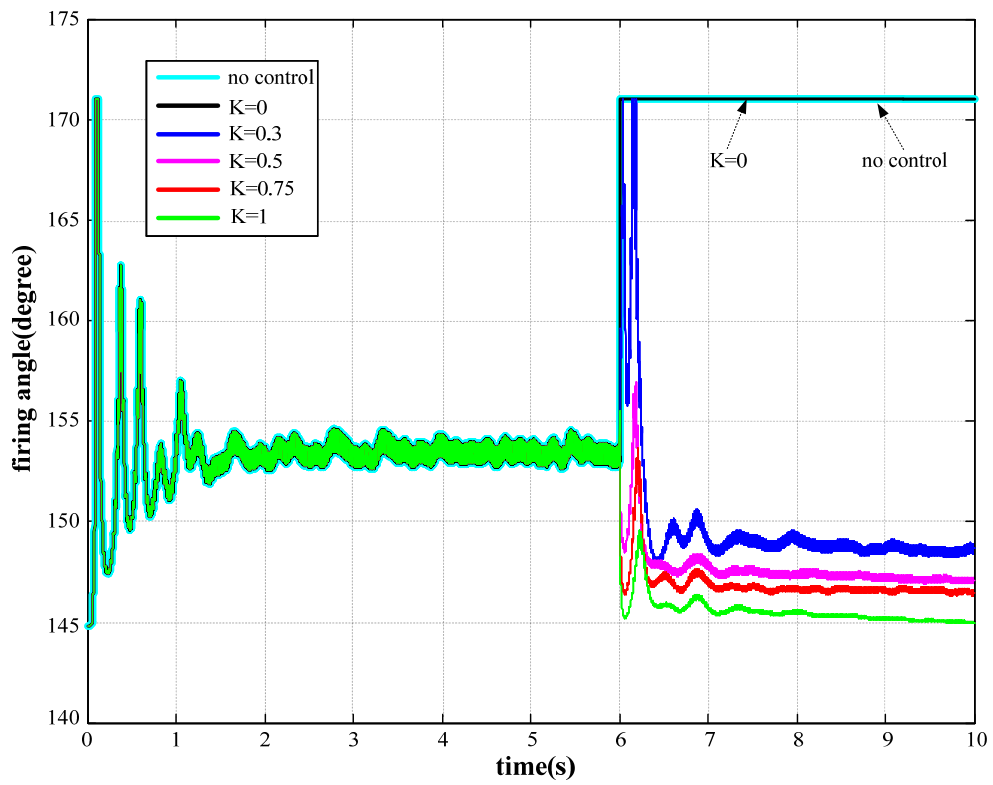
(d) Firing angle of TCSC
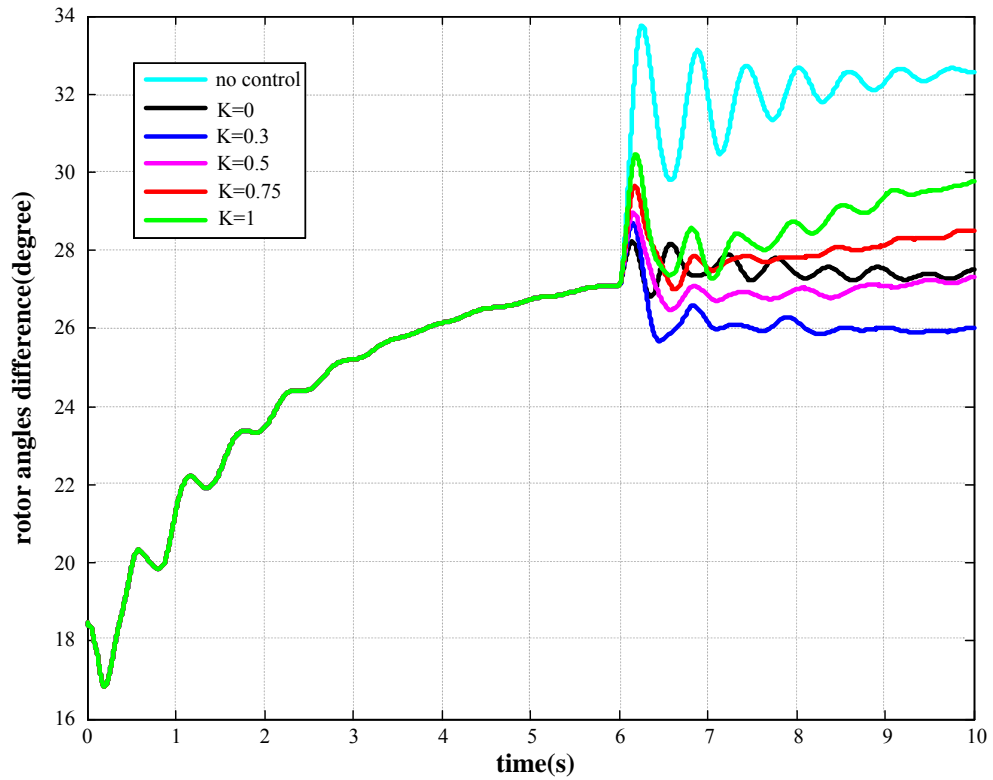
(e) Rotor angles reference

Figure 5.4 Comparison results of simulation

Parameter (Per Unit)	Pre-fault	Post-fault					
		No control	K=0	K=0.3	K=0.5	K=0.75	K=1
Line1(TCSC)	1.1	1.67	1.25	1.33	1.52	1.64	1.82
Line2	0.24	0.41	0.33	0.24	0.24	0.24	0.23
Line3	0.76	0	0	0	0	0	0
HVDC link	0.5	0.5	1	0.99	0.81	0.68	0.5
Northern Scotland generator	2.6	2.6	2.6	2.6	2.6	2.6	2.6

Table 5.1 Simulation results at pre-fault and post fault (S_{base}=1000MVA)

Conclusion

The coordinated control to re-dispatch the power flow and consequently improving the stability of power system is investigated through comparison of six cases in this chapter. A coordinated controller is designed to maintain total power flow transfer from one area to another area as constant as pre-fault. As applied power flow control devices, TCSC and HVDC link have different characteristics and advantages. TCSC can be controlled in lager range and HVDC link has more stable transmission ability. Because there are thermal, stability and voltage constraints of power system and limitations of TCSC and HVDC link, the optimum set-points of power flow controller should be studied and determined that the transient and dynamic stability of system is enhanced.

Chapter Six: Conclusions and recommendations for future work

The motivation and drive for the research were outlined in detail in previous chapters, as stemming from the fact that a substantial amount of change needs to be implemented to the GB transmission system in order to accommodate the forthcoming renewable generation and meet the climate change legislation enforced from both by UK Government. For that reason, more state-of-the-art transmission technologies such as embedded HVDC links and TCSC are planned to be deployed within the existing AC transmission system to provide additional capacity and raise the boundary limit. However, these new power flow control devices without a supervisory stability control system could bring less benefit of the potential advantages of these costly individual reinforcements. A coordinated controller is needed at transmission system level to ensure TCSC and LCC-HVDC link operate at the optimal operational point.

Chapter 2 presents a comprehensive review of the coordination of LCC-HVDC and FACTS devices. Several coordinated control methods are summarized. This research overview represents the first contribution of the thesis which reveals issues about coordination that deserve concern by researchers

This thesis in Chapter 3 covers and reviews the modelling of LCC- HVDC link and TCSC, which could be used for stability studies and analyzing complex system dynamic behavior. ADPSS software is used as the simulation tool for developing these models. The parameters of controllers are determined and validated by the step change tests.

As the second contribution of this thesis, applying power control of both TCSC and LCC-HVDC link in the simplified GB transmission system is simulated and studied in the Chapter 4. The simulation results illustrate the effect of two new technologies for improving the transient stability of power system. The obvious adverse interaction between two devices is not observed, but the coordinated control is still required to achieve better results in different conditions.

The most significant contribution of the research is to design a coordinated controller to maintain total power flow transfer from one area to another area as constant as pre-fault. In the Chapter 5, the coordinated control to re-dispatch the power flow at post-fault is applied different dispatched proportion to study the optimal operational point. Through the simulation analysis, HVDC link has very robust transmission reliability in controllable range which could pick up as much power flow as possible. TCSC has a large controllable range which can be mainly used to damp the oscillation. These two power flow control devices not only increase the power transfer capability but also enhance the transient stability effectively under this reasonable coordinated control.

The coordinated control for dispatching power flow in this thesis included two actuators (TCSC and HVDC link) which only contain a SISO (Single-Input Single-Output) power flow controller respectively. They are without any other function such as POD module and variables under two SISO controls may be easily coupled. There is no obvious interaction between TCSC and HVDC link when they operate under coordinated controller designed in this thesis. But they may be coupled while the new control functions add into individual actuators or other devices are embedded in power system. A new MIMO (Multi-Input and Multi-Output) controller should be designed in the future work to improve the performance of coordinated control. SR (Sampled Regulator) method, proposed by Åström [90], Lu and Kumar [91], and Mossaheb [92], is an efficient and feasible MIMO control design method. In [93], examples of the applications of the sampled integral regulators to some advanced FACTS devices have been reported. In [94], the application of HVDC link's set-point adoption is presented using a novel SR control design method for design of controller. Reference [95] reveals the essential relationship between the two different major designs for a class of samples regulator, which are Passive design and Lu-Kumar methods. The designs have been demonstrated through two power system applications, including power flow control using TCSC, coordination of HVDC power flow control and the SVC voltage regulation with the power damping control. According to these references, the coordinated control based on SR method will be studied if the research has been continued.

REFERENCES

[1] Ramesh, M., and A. Jaya Laxmi. "Stabilty of power transmission capability of HVDC system using FACTS controllers." Computer Communication and Informatics (ICCCI), 2012 International Conference on. IEEE, 2012.

[2] Padiyar, K. R. HVDC power transmission systems: technology and system interactions. New Age International, 1990.

[3] Rashid, Muhammad H. Power electronics handbook: devices, circuits and applications. Academic press, 2010.

[4] Setreus, J and Bertling, L, "Introduction to HVDC Technology for Reliable Electrical Power Systems" Proceedings of the 10th International Conference, 2006.

[5] R. Adapa, "High-wire Act: HVDC Technology: the state of the art," power and energy magazine, IEEE, no. October, pp. 18-29, 2012.

[6] Sood, Vijay K. HVDC and FACTS controllers: applications of static converters in power systems. Springer Science & Business Media, 2004.

[7] Larsson, Mats. "HVDC and HVDC light: An alternative power transmission system." Symposium on Control & Modeling of Alternative Energy Systems. 2009.

[8] Dodds, S., et al. "HVDC VSC (HVDC light) transmission–operating experiences." Proc. CIGRE Session, Paris, France (2010): 1-9.

[9] Kell, Dan. "HVDC to Grow Rapidly." Natural Gas & Electricity 31.10 (2015): 11-18.

[10] Anonymous, "HVDC Project List," Prepared for HVDC and Flexible AC transmission subcommittee of the IEEE Transmission and Distribution Committee, March 2012.

[11] Callavik, Magnus, Peter Lundberg, and O. Hansson. "NORDLINK Pioneering VSC-HVDC interconnector between Norway and Germany." ABB White Paper (2015).

[12] Oni, Oluwafemi E., Innocent E. Davidson, and Kamati NI Mbangula. "A review of LCC-HVDC and VSC-HVDC technologies and applications." Environment and Electrical Engineering (EEEIC), 2016 IEEE 16th International Conference on. IEEE, 2016.

[13] Neil Kirby. "HVDC Technology" Alstom Grid – IEEE PES T&D Expo, Chicago, April 2014

[14] Sellick, R. L., and Markus Åkerberg. "Comparison of HVDC Light (VSC) and HVDC Classic (LCC) site aspects, for a 500MW 400kV HVDC transmission scheme." (2012): 23-23.

[15] Kirby, N. M. "HVDC system solutions." Transmission and Distribution Conference and Exposition (T&D), 2012 IEEE PES. IEEE, 2012.

[16] Yinbiao Shu," Current Status and Development of National Grid of China", Transmission and Distribution Conference and Exhibition: Asia and Pacific, 2005 IEEE/PES.

[17] Naidoo, P, "Considerations for the Planning of UHVDC Schemes in Southern Africa" Power Engineering Society General Meeting, 2007. IEEE.

[18] Astrom, U., and Victor Lescale. "Converter stations for 800 kV HVDC." Power System Technology, 2006. PowerCon 2006. International Conference on. IEEE, 2006.

[19] Kumar, A., et al. "800 kV UHVDC–From Test Station to Project Execution." CIGRE Second International Symposium on Standards for Ultra High Voltage Transmission, New Delhi, India. 2009.

[20] Zehong, Liu, et al. "R&D progress of±1100kV UHVDC technology." B4-201-2012, CIGRE Session (2012).

[21] Liang Xuming, Ping Zhang, and Yong Chang. "Recent advances in high-voltage direct-current power transmission and its developing potential." Power System Technology 36.4 (2012): 1-9.

[22] Wen Jialinag, Wu Rui, and Peng Chang. "Analysis of DC grid prospects in China." High Voltage Engineering, 2012, 38(12): 3235-3239.

[23] Phillip G. Harris. "Key Convergences in the Global Electrical Industry." Presentation of the PES & IAS New York IEEE, April 28, 2016.

[24] "ENSG, 'Our Electricity Transmission Network: A Vision for 2020'' [Online]. Available on: https://www.gov.uk/government/uploads/system/uploads-/attachment_data/file/48274/4263-ensgFull.pdf, 02-02-2012.

[25] "DECC Energy Trends September 2016" [Online]. Available on: https://www.gov.uk/government/uploads/system/uploads/attachment_data/file/559574/Energy_Trends_September_2016.pdf, 29-10-2016.

[26] Lei, X., et al. "Coordinated operation of HVDC and FACTS." Power System Technology, 2000. Proceedings. PowerCon 2000. International Conference on. Vol. 1. IEEE, 2000.

[27] Zhang, Lidong, and Lars Dofnas. "A novel method to mitigate commutation failures in HVDC systems." Power System Technology, 2002. Proceedings. PowerCon 2002. International Conference on. Vol. 1. IEEE, 2002.

[28] Moreno, Rodrigo, Yanfei Chen, and Goran Strbac. "Evaluation of benefits of coordinated DC & AC flexible transmission systems with probabilistic security and corrective control." (2015): 27-6.

[29] Kunjumuhammed, L. P., R. Singh, and B. C. Pal. "Robust signal selection for damping of inter-area oscillations." IET generation, transmission & distribution 6.5 (2012): 404-416.

[30] Lee, R. L., et al. "Application of static var compensators for the dynamic performance of the Mead-Adelanto and Mead-Phoenix transmission projects." Power Delivery, IEEE Transactions on 10.1 (1995): 459-466.

[31] Beck, Günther, et al. "Use of FACTS and HVDC for Power System Interconnection and Grid Enhancement." POWER-GEN Middle East Conference, Jan30-Feb1. 2006.

[32] Waldhauer, H. "Grid Reinforcement and SVC for full Power Operation of Baltic Cable HVDC Link." The 38th Meeting and Colloquium of Cigré Study Committee B. Vol. 4. 2003.

[33] Retzmann, Dietmar, and Karl Uecker. "Benefits of HVDC & FACTS for sustainability and security of power supply." Powerafrica Conference and Exposition, Johannesburg. 2007.

[34] Yong, Jing, et al. "Digital simulation of AC/DC hybrid transmission system." Power System Technology, 2002. Proceedings. PowerCon 2002. International Conference on. Vol. 3. IEEE, 2002.

[35] Kirschner, L., D. Retzmann, and G. Thumm. "Benefits of FACTS for power system enhancement." Transmission and Distribution Conference and Exhibition: Asia and Pacific, 2005 IEEE/PES. IEEE, 2005.

[36] Zhang, Leiqi, et al. "Interaction assessment of FACTS control by RGA for the effective design of FACTS damping controllers." IEE Proceedings-Generation, Transmission and Distribution 153.5 (2006): 610-616.

[37] M. J. Gibbard, D. J. Vowles, and P. Pourbeik, "Interactions between and Effectiveness of Power Systems Stabilizers and FACTS controllers in Multi-Machine Systems," IEEE Trans. on Power Systems, Vol. 15, No. 2, pp. 748-755, May 2000.

[38] Kundur P., "Inter-area Oscillations in Power System," IEEE Power Engineering Society, pp. 13-16, October 1994.

[39] A. Kazemi, and B. Badrzadeh, "Modeling and Simulation of SVC and TCSC to Study Their Limits on Maximum Loadalibility Point," Electrical Power & Energy Systems, Vol. 26, pp. 619-626, 2004.

[40] Candelo, J. E., N. G. Caicedo, and F. Castro-Aranda. "Proposal for the solution of voltage stability using coordination of facts devices." Transmission & Distribution Conference and Exposition: Latin America, 2006. TDC'06. IEEE/PES. IEEE, 2006.

[41] Rajat Majumder, Bikash C. Pal, Christan Dufour, and Petr Korba, "Design and Real Time Implementation of Robust FACTS Controller for Damping Inter-Area Oscillation," IEEE Trans on Power Systems, Vol. 21, No.2, May 2006.

[42] L. J. Cai, and I. Erlich, "Simultaneous Coordinated Tuning of PSS and FACTS Damping Controllers in Large Power Systems," IEEE Trans. on Power Systems, Vol. 20, No. 1, February 2005.

[43] J. W. Park, R. G. Harley, and G. K. Vanayagamoorthy, "Power System Optimization and Coordination of Damping Controllers by Series FACTS Devices," Power Engineering Society Inaugural Conference & Exposition in Africa 2005, IEEE, 11-15 July, 2005, pp293-298.

[44] Karim Sebaa, and Mohamed Boudour, "Power System Dynamic Stability Enhancement via Coordinated Design of PSSs and SVC –based Controllers Using Hierarchical Real Coded NSGA-II," Power &Energy Society General Meeting – Conversion & Delivery of Electrical Energy in the 21st Century 2008, IEEE, 20-24 July, 2008, pp1-8.

[45] T. T. Nguyen, and R. Gianto, "Neural Networks for Adaptive Control Coordination of PSSs and FACTS Devices in Multi-machine power system," IET Gener. Transm. Distrib, 2008, Vol. 2, No. 3, pp355-372.

[46] Qing L, Zengzing W. Coordinated design of multiple FACTS controllers based on fuzzy immune co-evolutionary Algorithm[C]//2009 IEEE Power & Energy Society General Meeting. IEEE, 2009: 1-6.

[47] Juanjuan, Wang, Fu Chuang, and Zhang Yao. "Design of WAMS-based multiple HVDC damping control system." Smart Grid, IEEE Transactions on 2.2 (2011): 363-374.

[48] Gurrola, Aarón Esparza, Juan Segundo-Ramirez, and Ciro Nunez Gutierrez. "Wide area control in electric power systems incorporating FACTS controllers: Review." Power, Electronics and Computing (ROPEC), 2014 IEEE International Autumn Meeting on. IEEE, 2014

[49] Li, Yong, et al. "Robust Coordination of HVDC and FACTS Wide-Area Damping Controllers." Interconnected Power Systems. Springer Berlin Heidelberg, 2016. 121-135.

[50] Xu, Shiyun, et al. "A polytopic system theory approach to wide-area decentralized coordinated control of HVDC system." Cyber Technology in Automation, Control, and Intelligent Systems (CYBER), 2015 IEEE International Conference on. IEEE, 2015.

[51] HUANG Liuqiang, GUO Jianbo, SUN Huadong, XU Shiyun, LIU Min, YI Jun, China Electric Power Research Institute. "Wide-area anti-delay coordinated control among FACTS controllers." Electric Power Automation Equipment; 2014-01.

[52] Tian Fang, Li Yalou Zhou Xiaoxin, and et al. Advanced Digital power system simulator [J]. Power System Technology, 2008, 32(22): 17-22.

[53] User manual for Advanced Digital Power System Simulator. China Electric Power Research Institute, 2007

[54] Tian Fang, Li Yalou Zhou Xiaoxin, and et al. Research, development and application of advanced digital power system simulator (ADPSS)[C]. The International Conference on Electrical Engineering 2008, Okmawa, Japan, 2008.

[55] Zhi-hui, Liu, et al. "Modeling and simulation research of large-scale AC/DC hybrid power grid based on ADPSS." Power and Energy Engineering Conference (APPEEC), 2014 IEEE PES Asia-Pacific. IEEE, 2014.

[56] J. D. Ainsworth, "Proposed benchmark model for study of HVDC controls by simulator or digital computer," in Proc. CIGRE SC-14 Colloq. HVDC with Weak AC Systems, Maidstone, U.K., Sep. 1985.

[57] Faruque M O, Zhang Y, Dinavahi V. Detailed modeling of CIGRE HVDC benchmark system using PSCAD/EMTDC and PSB/SIMULINK[J]. IEEE transactions on power delivery, 2006, 21(1): 378-387.

[58] Prabha-Kundur, Power System Stability and Control, 1st ed. New York; McGraw- Hill.

[59] Dragan Jovcic and Khaled Ahmed, "High-Voltage Direct Current Transmission: Converters, Systems and DC Grids." Wiley 2015, 201AD. [60] CIGRE working group 14-29. "Coordination of controls of multiple FACTS/HVDC links in the same system." 1998.

[61] Hammad, A. E. "Stability and control of HVDC and AC transmissions in parallel." IEEE Transactions on Power Delivery 14.4 (1999): 1545-1554.

[62] XU Zheng, Dynamic Behavior Analysis of AC/DC Power System [M], Beijing: China Machine Press, 2000.

[63] Joshi, H. M., and N. H. Kothari. "A review on series compensation of

transmission lines and its impact on performance of transmission lines." Int J Eng Dev Res (2014): 72-76.

[64] S.R. Joshi, E.P. Cheriyan and A.M Kulkarni, "Output feedback SSR damping controller design based on modular discrete-time dynamic model of TCSC", Generation, Transmission & Distribution, IET, Vol: 3, no. 6, 2009, pp: 561 – 57.

[65] X.Zheng, Zheng Xu and Jing Zhang, "A Supplementary Damping Controller of TCSC for Mitigating SSR" Power & Energy Society General Meeting, 2009, PES '09, IEEE, pp. 1.

[66] K. R. Padiyar, "FACTS Controllers in Power Transmission and Distribution", Tunbridge Wells, Anshan, 2009.

[67] Hu, Guowen, Ming Cheng, and Guilong Cai. "Relation between fundamental frequency equivalent impedance and resonant point for thyristor controlled series compensation." Industrial Electronics Society, 2004. IECON 2004. 30th Annual Conference of IEEE. Vol. 2. IEEE, 2004.

[68] Nguyen, Tuan Anh, Dirk Van Hertem, and Johan Driesen. "A TCSC model for the power flow solution of the power transmission system of Vietnam." Universities Power Engineering Conference (UPEC), 2009 Proceedings of the 44th International. IEEE, 2009.

[69] Meikandasivam, S., and Shailendra Kumar Jain. "Behavioral Study of TCSC Device–A MATLAB/Simulink Implementation 1." (2008).

[70] Mathur, R. Mohan, and Rajiv K. Varma. Thyristor-based FACTS controllers for electrical transmission systems. John Wiley & Sons, 2002.

[71] N. Christl, R. Hedin, R. Johnson, P. Krause, and A. Montoya, "Power System Studies and Modeling for the Kayenta 230 kV Substation Advanced Series Compensation," IEE Fifth International Conference on AC and DC Power Transmission, London, September 1991.

[72] S. G. Jalali and R. H. Lasseter, "Harmonic Instabilities in Advanced Series Compensators," Proceedings of EPRI Conference on FACTS (FACTS 2), Boston, 1992.

[73] Del Rosso, Alberto D., Claudio A. Canizares, and Victor M. Dona. "A study of TCSC controller design for power system stability improvement." IEEE Transactions

on Power Systems 18.4 (2003): 1487-1496.

[74] Gama, Carlos, and Ricardo Tenorio. "Improvements for power systems performance: modeling, analysis and benefits of TCSCs." Power Engineering Society Winter Meeting, 2000. IEEE. Vol. 2. IEEE, 2000.

[75] Archana, N. V. "Adaptive controller strategies for FACTS devices in a power system to enhance stability." (2016).

[76] IEEE SSR working group. "First benchmark model for computer simulation of subsynchronous resonance." IEEE transactions on power apparatus and systems 96.5 (1977): 1565-1572.

[77] Kerahroudi, Shadi, Taylor G.A, F.Li, M.E.Bradley "Initial development of a novel stability control system for the future GB transmission system operation," Power Engineering Conference (UPEC), 2013 48th International Universities' , vol., no., pp.1,6, 2-5 Sept. 2013.

[78] S. K. Kerahroudi, G. A. Taylor, F. Li, and M. E. Bradley "Application of a Novel Stability Control System for Coordination of Power Flow Control Devices in the Future GB Transmission System" in EEE PES General Meeting, USA, Washington DC, July 2014, pp. 1–5.

[79] Anaya-Lara, O., F. M. Hughes, and N. Jenkins. "Generic network model for wind farm control scheme design and performance assessment." Network 1 (2005): C2.

[80] Ugalde-Loo, Carlos E., Janaka B. Ekanayake, and Nick Jenkins. "Subsynchronous resonance in a series-compensated Great Britain transmission network." IET Generation, Transmission & Distribution 7.3 (2013): 209-217.

[81] Zhaohua, Zeng, et al. "A Real-Time Simulation Study on Operation Mode of TCSC Varistor in Yiming-Fengtun 500 kV Power System." POWER SYSTEM TECHNOLOGY-BEIJING- 24.11 (2000): 23-27.

[82] L'Abbate, A., et al. "The role of facts and HVDC in the future paneuropean transmission system development." AC and DC Power Transmission, 2010. ACDC. 9th IET International Conference on. IET, 2010.

[83] Briscall, W. Brian, and Gerald C. Laxen. "Electrical line-fault detector and circuit breaker device." U.S. Patent No. 5,424,894. 13 Jun. 1995.

[84] Rugthaicharoencheep, N., T. Lantharthong, and S. Auchariyamet. "Optimal operation for active management of distribution system with distributed generation." Clean Electrical Power (ICCEP), 2011 International Conference on. IEEE, 2011.

[85] Swing, Power. "Out-of-Step Considerations on Transmission Lines." IEEE PSRC WG D 6: 2005.

[86] Thorp, James S., Charles E. Seyler, and Arun G. Phadke. "Electromechanical wave propagation in large electric power systems." IEEE Transactions on Circuits and Systems I: Fundamental Theory and Applications 45.6 (1998): 614-622.

[87] Martins, Nelson, Herminio JCP Pinto, and John J. Paserba. "Using a TCSC for line power scheduling and system oscillation damping-small signal and transient stability studies." Power Engineering Society Winter Meeting, 2000. IEEE. Vol. 2. IEEE, 2000.

[88] Pan, Mingsen, et al. "A coordination scheme of FACTS-based WADC to improve small signal stability with transient stability constraints in multi-machine system." Power & Energy Society General Meeting, 2015 IEEE. IEEE, 2015.

[89] Li, Yong, et al. "Robust Coordination of HVDC and FACTS Wide-Area Damping Controllers." Interconnected Power Systems. Springer Berlin Heidelberg, 2016. 121-135.

[90] K. J. Åström, "A robust sampled regulator for stable systems with monotone step responses," Automatica, vol. 16, no. 3, pp. 313–315, 1980.

[91] W.-S. Lu and K. S. P. Kumar, "A staircase model for unknown multivariable systems and design of regulators," Automatica, vol. 20, no. 1, pp. 109–112, 1984.

[92] S. Mossaheb, R. G. Cameron, and F. Li, "Passivity and the design of sampled regulators for uncertain systems," Int. J. Control, vol. 45, no. 6, pp. 1941–1952, 1987.

[93] Wang, H. F., and F. Li. "Multivariable sampled regulators for the co-ordinated control of STATCOM AC and DC voltage." IEE Proceedings-Generation, Transmission and Distribution 147.2 (2000): 93-98.

[94] Kerahroudi, Shadi Khaleghi, et al. "Power system stability enhancement of the future GB transmission system using HVDC link." Power Engineering Conference (UPEC), 2014 49th International Universities. IEEE, 2014.

[95] Kerahroudi, Shadi Khaleghi, et al. "Evaluating the Novel Application of a Class of Sampled Regulators for Power System Control." IEEE Transactions on Control Systems Technology 24.5 (2016): 1573-1581.

APPENDIX

♦ **Machine Data**

Southern Scotland					
Rating Capacity	3160 MVA	Base Voltage	33 kV	Base Frequency f_b	50 Hz
R_a	0.002	X_d	2.13	T'_{d0}	6.0857 s
X_l	0.17	X_d'	0.308	T''_{d0}	0.0526 s
X_q	2.07	X_d''	0.234	T''_{q0}	0.2538 s
X_q'	0.906	X_{mq}	1.9	T'_{q0}	1.653 s
X_q''	0.234	X_{md}	1.96		
Shaft Data					
Inertias (MWs/MVA) H_{SScot}		3.84	Damping coefficients (p.u. T/p.u. speed dev.) D_{SScot}		0.1

England and Wales					
Rating Capacity	21000 MVA	Base Voltage	33 kV	Base Frequency f_b	50 Hz
R_a	0.002	X_d	2.13	T'_{d0}	6.0857 s
X_l	0.17	X_d'	0.308	T''_{d0}	0.0526 s
X_q	2.07	X_d''	0.234	T''_{q0}	0.2538 s
X_q'	0.906	X_{mq}	1.9	T'_{q0}	1.653 s
X_q''	0.234	X_{md}	1.96		
Shaft Data					
Inertias (MWs/MVA) H_{EW}		5	Damping coefficients (p.u. T/p.u. speed dev.) D_{EW}		0.1

Northern Scotland					
Rating Capacity	2400 MVA	Base Voltage	33 kV	Base Frequency f_b	50 Hz
R_a	0.002	X_d	2.13	T'_{d0}	6.0857 s
X_l	0.17	X_d'	0.308	T''_{d0}	0.0526 s
X_q	2.07	X_d''	0.234	T''_{q0}	0.2538 s
X_q'	0.906	X_{mq}	1.9	T'_{q0}	1.653 s
X_q''	0.234	X_{md}	1.96		
Shaft Data					
Inertias (MWs/MVA) H_{NS}	3	Damping coefficients (p.u. T/p.u. speed dev.) D_{SSc}		0.1	

- ◆ **DC System (Mono-pole and 12 pulses):**

Converter Data					
Rating Capacity	1000MVA	Base Voltage	500 kV	Base Frequency f_b	50 Hz
DC Transmission Line and Inductor					
Inductor	0.5968 H	Line Resistance	5 Ω	Capacitance	26.0μF
Converter transformer Rectifier					
Rating Capacity		603.73MWA	Leakage Reactance		0.18p.u
Voltage Ratio		400/213.57kV			
Converter transformer Inverter					
Rating Capacity		591.79MWA	Leakage Reactance		0.18p.u
Voltage Ratio		400/209.2288kV			

- **AC system for Chapter Four**

Transformer and transmission lines					
Rating Capacity	1000MVA	Base Voltage	400 kV	Base Frequency f_b	50 Hz
X_{T1}	0.14	X_{T2}	0.07	X_{T3}	0.00001
Line1	0.1	*Line2*	0.1	*Line3*	0.05
Line4	0.01		Shunt capacitances X_{CSh}		20 p.u.
A ratio $X/R = 10$ is assumed					
Load					
P_{Load}		18.23	Q_{Load}		2.4847
P_{Load1}		2.0	Q_{Load}		0

- **AC system for Chapter Five**

Transformer and transmission lines					
Rating Capacity	1000MVA	Base Voltage	400 kV	Base Frequency f_b	50 Hz
X_{T1}	0.14	X_{T2}	0.07	X_{T3}	0.00001
Line1	0.1	*Line2*	0.4	*Line3*	0.15
Line4	0.01		Shunt capacitances X_{CSh}		20 p.u.
A ratio $X/R = 10$ is assumed					
Load					
P_{Load}		18.23	Q_{Load}		2.4847
P_{Load1}		2.0	Q_{Load}		0